UNIVERSITÀ DEGLI STUDI DELL'INSUBRIA

Ph.D. School:

Biological and Medical Sciences

Ph.D. Course:

Analysis, Protection and Management of Biodiversity

XXIV cycle

Coordinator: Prof. Marco Saroglia

SILKWORM LARVAL MIDGUT:
A STRIKING EXAMPLE OF TISSUE REMODELING

Supervisors:

Prof. Roberto Valvassori

Prof. Gianluca Tettamanti

Candidate:

Dr Eleonora Franzetti

ACADEMIC YEAR 2010-2011

INDEX

ABSTRACT

Bombyx mori is a pivotal model organism among Lepidoptera, a group of insects that is important for both commercial and agronomic purposes. The study of midgut development during larval period and metamorphosis is helpful to obtain a background useful for many applications concerning these contexts.

In these insects, metamorphosis involves a series of highly ordered mechanisms and passes through a well-defined sequence of events to eliminate tissues and organs that are functional only in larval stages (Meléndez and Neufeld, 2008). In Lepidoptera, midgut tissue undergoes extensive remodelling (Vilaplana et al., 2007) during the development and these modifications lead to cell death of the larval epithelium and to its replacement with a new pupal epithelium, which becomes the adult midgut epithelium. For this reason midgut remodelling has been chosen as preferential model to study cell death mechanisms and regeneration processes, and their regulation. In particular, although features of apoptosis and autophagy have been reported in the larval organs of Lepidoptera during metamorphosis, solid experimental evidence for autophagy is still lacking. Moreover, the role of the two cell death processes and the nature of their relationship are still cryptic.

In order to analyze the remodelling processes in *B. mori* midgut tissues during larval-adult transformation, we performed a morpho-functional analysis at different developmental stages. In addition, we accomplished a cellular, biochemical and molecular analysis of the degeneration process that occurs in the larval midgut, with the aim to analyze autophagy and apoptosis in cells that dye under physiological conditions.

We found that stem cells proliferate actively since the wandering stage, leading to the formation of a new pupal midgut which is progressively remodelled until adult ecdysis. Larval midgut cells undergo progressive degradation, forming a compact mass called yellow body, that progressively degenerates inside the lumen of the new pupal midgut and finally disappears.

Through histochemical analysis we showed marked changes in metabolic activity in both larval and pupal epithelium at different stages of the midgut renewal process.

We demonstrated that larval midgut degradation is a gradual process due to the concerted action of autophagic and apoptotic mechanisms, which occur at different times and have different functions. In particular, autophagy is activated from the wandering stage and reaches a high level of activity during the spinning and prepupal stages. Our data showed also that the process of autophagy can recycle molecules from the degenerating cells and supply nutrients to the animal during the non-feeding period. Apoptosis intervenes later. In fact, although genes encoding caspases are transcribed at the end of the larval period, the activity of these proteases is not appreciable until the second day of spinning and apoptotic features are observable from prepupal phase. The abundance of apoptotic features during the pupal phase, when the majority of the cells die, indicates that apoptosis is actually responsible for cell death and for the disappearance of larval midgut cells.

INTRODUCTION

Lepidoptera are holometabolous insects with life cycle consisting of four stages: egg, larva or caterpillar, pupa or chrysalis and imago or adult.

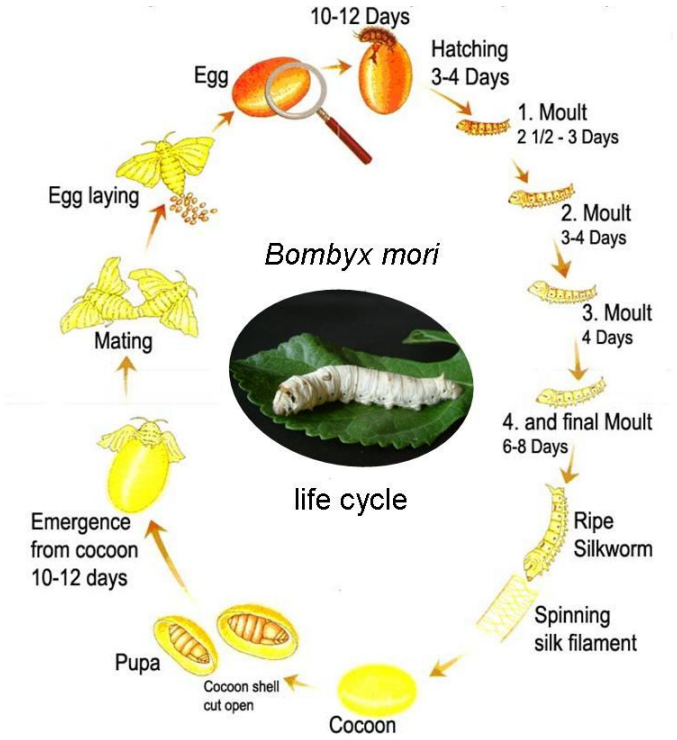

Fig. 1. *Bombyx mori* life cycle.

The larvae spend much of their time feeding and grow very quickly going through a series of phases (i.e. instars). The fully matured larva spins a cocoon in which it is encapsulated, forming the pupa or chrysalis. Once emerged, the adults are mainly occupied in mating. The egg laying takes place near or on the preferred plant, thus ensuring food supply for the new generation of larvae.

Lepidoptera play an important role in the natural ecosystems for their efficient foraging strategies as phytophagous on live plant matter and for their role in the pollination activity. Several species are of economic interest both for their silk product and for their role as pest insects. In this context many lepidopteran larvae are considered as pest insects due to the massive damages caused to cultivated crops and vegetation. Thus a lot of researches are focused on methods for pest insects

control (Chapman, 1998; Levy et al., 2004) using integrated strategies of management (Zanuncio et al., 1994).

To improve the understanding of the morpho-physiological mechanisms involved in the development and growth of the pest species, cellular and molecular analyses are required. In fact an increase in the effectiveness of the techniques used in the control of the dangerous species could reduce, or even avoid, the massive use of chemical insecticides, thus preventing the development of resistant strains and minimizing the environmental impact related to the generalized toxic effects to both invertebrates and vertebrates (Zanuncio et al., 1994, 1996, 1996-1997).

On the other hand it is attractive for many applications, the chance to acquire a greater knowledge about insects of considerable agronomic interest such as those species reared for commercial purposes, as the silkworm *Bombyx mori*. This animal is an important source of livelihood for subsistence farmers engaged in silk production in many countries and thus resulting in a consequent benefit to the textile industry (Wang et al., 2005). Hence the increase of information about the fine morphological events and molecular regulation of the developmental processes during metamorphosis could facilitate studies on several economic and therapeutic applications.

Silk is a mechanical robust bio-material with environmental stability, bio-compatibility and bio-degradability, which also offers a wide range of practical properties for bio-medical applications (Reddy and Prasad, 2011) and silk produced by *B. mori* provides an important set of options for bio-materials because of its good thermal and mechanical properties. For innovative and advanced functional biological applications, the modern applied research offers the possibility of utilizing transgenic silkworms as a valuable tool for the production of nutritional, cosmetic, pharmaceutical, bio-medical and bio-engineering products.

B. mori is also considered a pivotal model to organize biological knowledge for other lepidopterans (Wang et al., 2005) because of the indisputable advantages due to a large number of information gathered on its developmental biology, physiology and endocrinology, for the availability of numerous genetic and molecular biology tools and for a completely sequenced genome. In particular, techniques for efficient gene transfer (stable germline transformation through transposon-based vectors or

transient expression of genes by using virus vectors) or gene silencing (RNAi) have been developed for this species in the last ten years (Malagoli et al., 2010).

Alimentary canal of Lepidoptera: structure, physiology and development

Lepidoptera have life and feeding styles different from dipteran, hymenopteran and coleopteran insects (Tanaka et al., 2008); moreover their alimentary canal may be different from species to species or even during life stages of the same animal (Hakim et al., 2010).

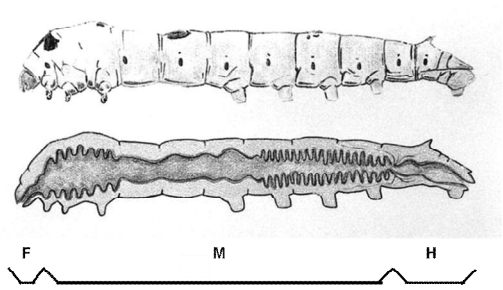

Fig. 2. Digestive tract of lepidopteran larvae can be divided into three different regions. F, foregut; M, midgut; H, hindgut. (Giordana et al., 1998).

In these insects, alimentary canal is composed of three regions: the foregut, the midgut, and the hindgut (Uwo et al., 2002). The foregut and the hindgut are short portions. The first is considered a vestigial apparatus (Crowson, 1981), and leads straight into the midgut (Dow, 1986), while the hindgut is subdivided in an anterior region (ileum), where the solid material is squeezed of excess fluid, and in a posterior part (rectum), where the undigested materials passes out through the anus (Dow, 1986).

In the larvae the midgut represents the middle region of the digestive tract and occupies most of the body cavity. It is a complex structure that carries out digestive and absorptive functions (Dow, 1986). It is lined by several layers of a delaminated peritrophic membrane, which has a fundamental role of protection because it is positioned between the gut lumen and the epithelial layer; it works by preserving the epithelium from mechanical damage and bacterial infection, as a barrier against toxins and harmful insecticides (Terra, 2001), as well as plays a selective role in the passage of nutrients (Tettamanti et al., 2011).

This organ consists of a highly folded monolayered epithelium, which is supported by a basement membrane, striated muscles, and tracheoles.

There are three morphologically distinct regions in the lepidopteran midgut, with functional specializations for water movement or nutrient absorption (Dow, 1986):

ultrastructural and enzyme evidence suggests that the anterior-middle midgut is specialized for absorption of nutrients and displays the presence of digestive enzymes, while the posterior midgut is involved in retention of water (Santos et al., 1984).

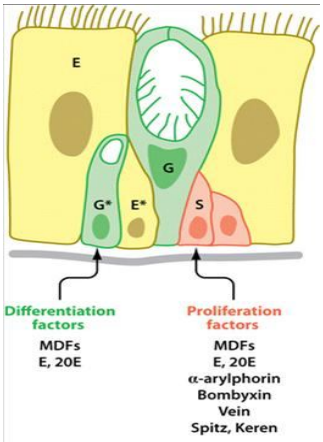

Figura 3. Factors involved in larval stem cell proliferation and differentiation. E, columnar cell; G, goblet cell; S, stem cell; E*, developing columnar cell; G*, developing goblet cell. (Hakim et al., 2010).

Midgut epithelium is composed by four cell types, morphologically and functionally distinct. The prevalent cell types, present along the entire length of the midgut (Dow, 1986), are goblet and columnar cells, which are involved in secretory activity and nutrient uptake, respectively.

The mature columnar cells are responsible for the absorption of nutrients (Terra and Ferreira, 2005; Giordana et al., 1998; Leonardi et al., 1998; Casartelli et al., 2001). Their apical membranes form a brush-border, while the basal membrane is extensively folded. The basal infoldings may extend beyond the mid-height of the cell, where the nucleus and numerous compartmentalized mithocondria are located. The cytoplasm contains abundant rough endoplasmic reticulum, microtubules distributed mainly in intermediate and apical regions, and actin filaments localized in the apical and microvillar area (Barbehenn and Kristensen, 2003).

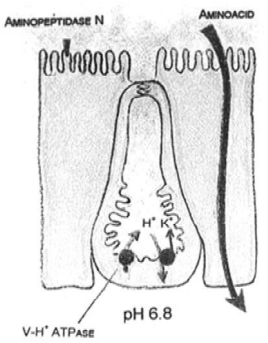

Fig.4. At the microscopic level, a vacuolar-type proton ATP-ase and a $K^+/2H^+$ antiporter in the membrane lining the goblet cavity are involved in the drastic alkalinization of the midgut lumen, required for the proper funtioning of the epithelium (Giordana et al., 1998).

Goblet cells are a peculiar cell type involved in the ionic homeostasis of the midgut (Wieczorek et al., 2000). Goblet cells show a large intracellular cavity that communicates with the lumen via a long “neck”. Microvilli line the cavity and contain mithocondria and electron-dense bodies known as portasomes (Giordana et al., 1998; Barbehenn and Kristensen, 2003) in which vacuolar-ATPase (V-ATPase) is involved in the transport mechanism, basic for the alkalinization and for the maintainance of high potassium concentration of the midgut lumen (Barbehenn and Kristensen, 2003). Interspersed

between columnar and goblet cells there are small stem cells organized in clusters resting at the base of the mature cells. They are able to differentiate into columnar and goblet cells (Baldwin et al., 1996; Hakim et al., 2010). Few and scattered endocrine cells have been indentified in the epithelium (Endo and Nishiitsutsuji-Uwo, 1981), localized in the basal region. These cells secrete a wide variety of hormones which play a role in differentiation of stem cells and in the control of digestive enzyme secretion (Wigglesworth, 1972).

Stem cells not only take part to the growth of the midgut epithelium during larval-larval moults, but they also set in motion to repair this tissue following damage; in addition, at pupal stage stem cells play a key role in the generation of the midgut of the adult, that in these holometabolous insects is characterized by different food habits (Tettamanti et al., 2007a; Hakim et al., 2010).

In those species where feeding habits change dramatically from larva to adult, it is extremely important that, during insect metamorphosis, midgut tissue undergoes extensive remodelling (Vilaplana et al., 2007).

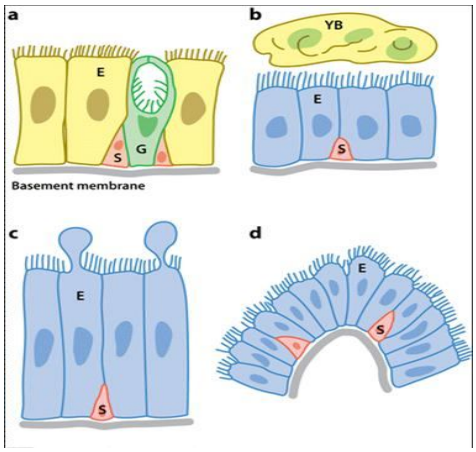

Fig. 5. The midgut epithelium during different stages of the life cycle of a lepidopteran. E, columnar cell; G, goblet cell; S, stem cell; YB, yellow body. (Hakim et al., 2010).

Midgut remodelling in insects consists of two main events: proliferation and differentiation of stem cells to form pupal/adult midgut epithelium and cell death of larval midgut epithelium (Parthasarathy and Palli, 2007b).

In fact, during metamorphosis, the growth of the pupal midgut epithelium occurs concomitantly with the discharge of the larval epithelium, that forms a compact mass called yellow body (Wigglesworth, 1972), into the gut lumen where it undergoes a progressive demise (Tettamanti et al., 2007a).

Factors and hormones that regulate midgut remodelling

In insects, moults and metamorphosis are regulated by hormones (Judy and Gilbert, 1970; Waku and Sumimoto, 1971; Humbert, 1979; Baldwin and Hakim, 1991; Jiang

et al., 1997; Uwo et al., 2002; Martins et al., 2006). These play an important role in development, reproduction, metabolism, and homeostasis.

In holometabulous insects the replacement of midgut during larval-adult transformation is a hormone dependent tissue remodelling event (Nishiura and Smouse, 2000; Lee et al., 2002; Cakouros et al., 2004; Daish et al., 2004; Wu et al., 2006) and is regulated by the changes in the titer of steroid hormone, 20-hydrossxyecdysone (20E) and related molecules. A pulse of 20E at the end of the last larval stage triggers the onset of prepupal development. A second pulse of 20E initiates pupation (Riddiford, 1993). The juvenile hormone (JH) is released steadily over time and ensures the growth of the larva, while preventing metamorphosis (Riddiford et al., 1990). When JH levels drop, the major event occurring during midgut remodeling is the activation of gene expression by 20E (Wu et al., 2006). 20E activates the genes that regulate metamorphosis in a hierarchical way, thus leading to the final transformation from pupa to adult. Thus there is a finely tuned balance of 20E and JH (Hakim et al., 2010).

20E and JH act mainly on proliferation and differentiation of lepidopteran stem cells (Sadrud-Din et al., 1994, 1996; Lee and Baehrecke, 2001; Lee et al., 2002; Wu et al., 2006; Parthasarathy and Palli, 2007a, b; Hakim et al., 2010), and 20E can even induce apoptosis (Terashima et al., 2000; Fahrbach et al., 2005).

Several factors contribute to the regulation of stem cell proliferation and differentiation. In larvae of *Drosophila melanogaster* it has been clearly demonstrated that epidermal growth factor receptor (EGFR) stimulates adult midgut stem cells to proliferate (Jiang and Edgar, 2009). In the early larval instars, the surrounding midgut visceral muscles produce the protein Vein, a weak EGFR ligand, which stimulates a low level of adult midgut precursor cell proliferation via a paracrine pathway. Subsequently, two other ligands are synthesized by stem cells themselves; these provide autocrine signals that augment the paracrine signal. The combination of signals leads to a higher level of proliferation in the late period.

At least together with 20E, independent mitogens control the growth in the midgut (Hakim et al., 2010). In Lepidoptera midgut cells, α-arylphorin and bombyxin function as mytogens and stimulate proliferation and differentiation. Analysis *in vitro* suggests that midgut differentiation factors (MDF1 and MDF2), purified from a conditioned

medium in which larval midgut cells have been cultured, are present in enterocytes exhibiting a local control over proliferation and/or differentiation during larval molting. This local control mechanism may also function during midgut repair, after injury (Spies and Spence, 1985).

Several studies support the issue that also nutrition controls stem cells function. In starved *Periplaneta americana*, stem cell proliferation decreases along with the size of the midgut. After refeeding, the proliferation rate rebounds (Park and Takeda, 2008). In fact, massive gut remodelling mainly occurs in response to the need of nutrients during the pupal period and for the renewal of an organ that will have to fulfil adult alimentary requirements (Wigglesworth, 1972; Dow, 1986).

Cell death

Development and tissue homeostasis is a delicate balance between cell proliferation and cell death (Cooper et al., 2009; Ulukaya et al., 2011) and different modalities of cell death play a critical role generally in body remodelling during the development and metamorphosis of holometabolous insects to eliminate tissues and organs that are functional only in embryonic and larval stages (Meléndez and Neufeld, 2008).

Cell death represents a highly heterogeneous process that can follow the activation of distinct (although sometimes partially overlapping) biochemical cascades and it appears with different morphological features. In fact the Nomenclature Committee on Cell Death has recently furnished detailed recommendations and descriptions about several mechanisms that induce cell death in eukaryotes (Kroemer et al., 2009; Galluzzi et al., 2012) and three major subtypes based on morphological criteria have been classified (Malagoli et al., 2010): apoptosis, autophagic cell death, necrosis. Mixed cell death morphotypes characterized by traits of these three mechanisms have also been reported (Galluzzi et al., 2009).

In multicellular organisms, the timely execution of cell death is critical for numerous physiological processes including embryogenesis, post-embryonic development and adult tissue homeostasis (Galluzzi et al., 2009).

Apoptosis and autophagy are the two most prominent morphological forms of cell death that occur during animal development processes (Schweichel and Merker, 1973; Clarke, 1990). Studies on *Heliothis virescens* (Tettamanti et al., 2007b) and

Spodoptera frugiperda (Vilaplana et al., 2007) larvae, demonstrated that the destruction of the larval midgut epithelium is accomplished by the combined action of apoptosis (Parthasarathy and Palli, 2007a, b), and autophagy events, which are detected within the degenerating yellow body (Kőműves et al., 1985; Jiang et al., 1997; Lee and Baehrecke, 2001; Lee et al., 2002; Uwo et al., 2002; Wu et al., 2006; Parthasarathy and Palli, 2007b). The occurrence of the self-digestion process is supported by the presence of the typical morphological characters, by the detection of a striking increase of lysosomal enzymes (Tettamanti et al., 2007b), and by the formation of autophagic vacuoles that are used for cytoplasmic destruction (Sumithra et al., 2010). The involvement of autophagy in the removal of midgut in Lepidoptera has been assessed recently, although its role is quite troublesome (Tettamanti et al., 2007a).

Apoptosis

Apoptosis is known to be the classical mechanism of cell death (Cotter et al., 1990). In the literature, the term "apoptosis" has been first used by Kerr et al. (1972) and was defined to describe a specific morphological aspect of cell death (Kroemer et al., 2009).

Apoptosis is accompanied by reduction of cellular volume (pyknosis), chromatin condensation, nuclear fragmentation (karyorrhexis), little or no ultrastructural modifications of cytoplasmic organelles, and plasma membrane blebbing (but maintenance of its integrity until the final stages of the process) (Kroemer et al., 2009). The deceased cell is packaged into apoptotic bodies, that are removed by phagocytic cells (Edinger and Thompson, 2004).

The role of apoptosis is significant in many physiological processes, such as in normal cell turnover, in cytotoxic functions of the immune system (Ulukaya et al., 2011), and in developmental biology, for instance in the embryonic development of tissues and organs and the formation of limbs (Clarke, 1990), in the development of the nervous system (Batistaou and Greene, 1993; Johnson and Deckwerth, 1993), and in hormone-dependent tissue remodeling (Strange et al., 1992).

During animal growth, excess of cells are generated during the development of a number of organ systems, and the control of cell numbers during development is

critical for the size of tissues and organs. The deletion of cells no longer needed by apoptosis is a common feature of development in animals and may be necessary for its proper progression. For example, apoptosis is a critical aspect of the development of the vertebrate nervous system and much more the removal of the larval salivary gland during *Drosophila melanogaster* metamorphosis is probably the best-understood example of this type of cell death (Conradt, 2009).

Apoptosis is finely controlled at the molecular level. It is characterized by the activation of caspases, although a caspase-indipendent of apoptosis pathway also exists, and involves apoptosis-inducing factors (AIFs), which are released from the mithocondria into the cytosol and traslocated to the nucleus (Ulukaya et al., 2011).

Caspases activate each other, resulting in a cascade of proteolytic reactions. Some caspases are known as initiator caspases (caspase 2, 8, 9 and 10), whereas the others are effector caspases (caspase 3, 6 and 7). Initiator caspases transmit the death signal generated by the apoptotic stimulus to effector caspases, which act to cleave the target proteins and thus produce the morphological features of apoptosis (Ulukaya et al., 2011).

The type of caspase expressed by a given tissue may vary and cells may require activation of various caspases in the different steps of differentiation (Ulukaya et al., 2011). Nevertheless, caspase-3 is the universal caspase that functions almost in all tissues.

Various caspase inhibitors are known. These inhibitors are the members of a large family of inhibitor of apoptosis proteins (IAPs), which inhibit caspases selectively and halt the apoptotic process (Ulukaya et al., 2011), thus taking the role of key regulators of cell death (Vilaplana et al., 2007). A combination of IAPs and caspases affects the balance of apoptotic processes.

Caspases have been identified in many different organisms ranging from mammals (11 caspases in human and 10 in mice), to nematodes (3 caspases) (Lamkanfi et al., 2002); therefore it is not surprising that these proteins have been found in all metazoans, including insects (Cooper et al., 2009).

The conservation of structural and biochemical properties of caspases found in metazoans underlines the importance of these enzymes in the cell death process (Cooper et al., 2009).

Since the role of human caspases is complex, crucial insights can be gained from the study of similar molecules in other models, including insects, where apoptosis occur under both physiological and pathological conditions.

Autophagy

Autophagy is a ubiquitous catabolic process that involves the bulk degradation of cytoplasmic components through a lysosomal pathway (Meléndez and Neufeld, 2008). The term autophagy usually refers to macroautophagy, although three types of autophagy are known, that are macroautophagy, microautophagy and chaperone-mediated autophagy (Tettamanti et al., 2011).

This process is characterized by the engulfement of part of the cytoplasm inside a membrane, called phogophore or isolation membrane, that progressively expands and finally closes forming a double membrane structure, called autophagosome (Tettamanti et al., 2011). Autophagosomes are delimited by a double membrane and contain degenerating cytoplasmic organelles or cytosol (Kroemer et al., 2009). Once the autophagosome membrane fuses with lysosomes generates autolysosomes, in which both autophagosome inner membrane and its luminal content are degraded by acidic lysosomal hydrolases (Kroemer et al., 2009), and the resulting macromolecules are recycled back into the cytosol (Mizushima et al., 2008) for macromolecular synthesis and/or ATP generation (Chang and Neufeld, 2010). This catabolic process marks the completion of the autophagic pathway.

Although autophagy, as a cellular self-eating process, can potentially degrade cytoplasmic proteins and any organelles, selective organelle degradation has been described in yeast and other cell models. Pexophagy (Manjithaya et al., 2010), mitophagy (Narendra et al., 2008), nucleophagy (Park et al., 2009) and reticulophagy (Bernales et al., 2007) are responsible for specific dismantling of peroxisomes, mithocondria, nucleus and endoplasmic reticulum, respectively.

All the steps required for the formation of the autophagosomes up to the final degradation and re-export of material to the cytoplasm, are regulated by a controlled mechanism involving a series of Atg proteins coded by autophagy-related genes (*ATG*).

The molecular cascade that regulates autophagy can be dramatically up-regulated by a number of stimuli. Since autophagy is inhibited under nutrient-rich conditions, the best characterized of these stimuli is nutrient starvation, which induces autophagy in part through the inactivation of the protein kinase target of rapamycin (Tor) (Meléndez and Neufeld, 2008). All the conjugation systems that act to create the functional complexes to achieve all the several steps in which the autophagic process can be divided, have an essential role in autophagy and they are widely conserved in eukaryotes: they are involved in signaling and induction, autophagosome nucleation, membrane expansion vesicle completion, autophagosome targeting, docking and fusion with the lysosome, and, finally, degradation of the cargo within the newly formed autolysosomes (Meléndez and Neufeld, 2008).

Genomic analysis in various model organisms revealed genes involved in the inductive step of the autophagic pathway or in autophagosome formation, thus suggesting a strong conservation of these conjugation systems (Malagoli et al., 2010).

In *B. mori* genome there are homologs of most of the *ATG* genes originally identified in yeast and subsequently in higher eukaryotes (Zhang et al., 2009). Along with 11 *ATG* genes, two paralogous Target of rapamycin (*TOR*) genes have been identified: *BmTOR1* and *BmTOR2* (Zhou et al., 2010), and most of these genes are involved in the two ubiquitin-like conjugation systems, Atg8-PE and Atg12-Atg5-Atg16. The expression of the genes for the ubiquitin-like conjugation systems (including BmAtg3, BmAtg4, BmAtg8 and BmAtg12), and for the formation of autophagosomes (including BmAtg1, BmAtg6 and BmAtg18) were detected in the silk gland of *Bombyx mori*.

However, autophagy is a physiological process that plays a homeostatic role and can be rapidly up-regulated when the organism is undergoing architectural remodelling, in which case it allows an adequate turnover of the cell components in most tissues (Lockshin and Zakeri, 2004; Tettamanti et al., 2011). The occurence of extensive autophagy is usually explained by the need to destroy entire tissues during development (Yin and Thummel, 2005). Thus autophagy is usually associated with developmental, differentiation and tissue remodelling processes, such as in insect metamorphosis (Tettamanti et al., 2011).

Autophagy seems also to have a key role in cell death processes (autophagic cell death) (Jiang et al., 1997; Lee and Baehrecke, 2001; Lee et al., 2002; Kroemer and

Levine, 2008; Eisenberg-Lerner et al., 2009). However this issue is still under debate (Kroemer and Levine, 2008) and the reappraisal of some experimental models suitable for studying autophagy (Klionsky, 2007), such as Lepidoptera, could give useful insights about this issue.

Cross-talk between apoptosis and autophagy

Apoptosis and autophagy are not mutually exclusive pathways. These two processes, which appear to share certain common regulatory pathways, may interact in a variety of ways, depending upon the cellular environment and the treatments performed (Sadasivan et al., 2006).

This overlap between apoptotic and autophagic cell death programs and the evidence that some morphological, biochemical and molecular features are not exclusive to either autophagy or apoptosis (Berry and Baehrecke, 2007; Nezis et al., 2010) have led to a search for possible mediators common to these two processes. The involvement of active caspases is also under investigation, since it does not seem to be a feature exclusively linked to apoptosis (Tettamanti et al., 2011). Moreover, some authors reported the intervention in self-digesting processes of other factors, such as IAP, whose expression modifies during midgut remodelling in Lepidoptera (Parthasarathy and Palli, 2007b; Vilaplana et al., 2007) and during the development in *Drosophila* (Hou et al., 2008). The data could provide a mechanistic link between autophagy and apoptosis to achieve cell ceath (Nezis et al., 2010).

Among the autophagic genes, *ATG5* has been suggested to be a molecular link between autophagy and apoptosis in mammals, since it plays a role in autophagosome formation, and is also involved in a pro-apoptotic signalling pathway through cytochrome c release and caspase activation (Yousefi et al., 2006).

Eisenberg-Lerner et al. (2009) analyzed the synergy between autophagy and apoptosis and observed that the co-occurrence of autophagy and apoptosis within the same tissue represents a cooperation to lead to cell death. In this way autophagy could work as a back-up system to ensure cell death if the apoptotic process failed, but it could also establish a partnership with apoptosis to maximize the death process. Alternatively, autophagy and apoptosis would act as a pro-survival mechanism that helps cells to maintain homeostasis until a point of no return, after

which apoptosis is activated and cell dies. A third possibility is that autophagy may enable apoptosis by participating in the regulation of some molecular mechanisms of the apoptotic machinery. Although all three of the hypotheses can be envisaged for Lepidoptera, the current lack of sufficient information about the molecular mechanisms underpinning the interconnection between apoptosis and autophagy, and the complexity of the phenotypic features evidenced in the dying tissues in the larvae, do not yet allow us to disentangle this problem (Tettamanti et al., 2011).

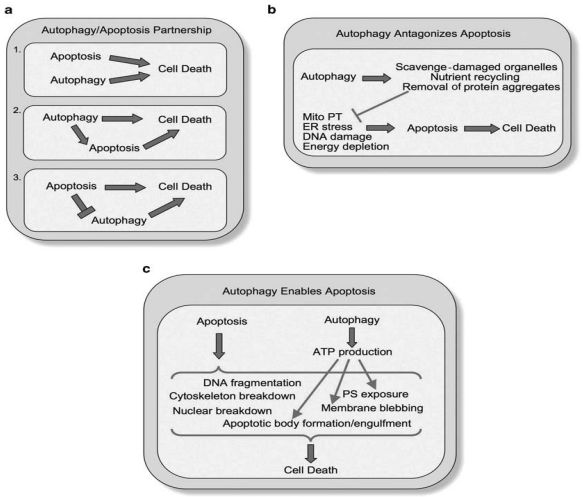

Fig. 6. Cross-talk between apoptosis and autophagy (Eisenberg-Lerner et al., 2009).

GOAL OF THE RESEARCH

Lepidoptera midgut is an ideal *in vivo* model system for studying cell death. In fact, during metamorphosis, the larval midgut epithelium degenerates and the cells die. The cell death pathways in this organ still need to be elucidated.

This study focuses on the remodelling processes in midgut tissues during larval-adult transformation in the silkworm, *Bombyx mori*, to obtain:

- a morpho-functional characterization of the midgut at different developmental stages during the midgut renewal process;
- a detailed analysis of the cell death mechanisms that lead to the disappearance of the larval midgut epithelium during the degeneration process. This analysis is achieved through multiple assays, as recommended by the most recent guidelines.

MATERIALS AND METHODS

Experimental animals

B. mori (four-way polyhybrid strain (126x57)(70x90)) larvae were provided by CRA-API (Padova, Italy). The larvae were fed with artificial diet (Cappellozza et al., 2005) and reared at 25 ± 0.5°C under a 12L:12D photoperiod and 70% relative humidity. After animals had ecdysed to the last larval stage (fifth instar), they were staged and synchronized according to Kiguchi and Agui (Kiguchi and Agui, 1981). Developmental stages used in this study are defined and described in Table 1.

Table 1. Definition and description of developmental stages of the silkworm, *Bombyx mori*, used in this study

Stage	Definition	Midgut description
L5D1-L5D5	Fifth larval instar day 1 - day 5	The larval midgut epithelium is well-organized
W (S)	Wandering stage / early spinning	The larval midgut epithelium is well-organized. Stem cells start to proliferate
SD1	Spinning stage day 1	The larval midgut epithelium starts to degenerate. Proliferation of stem cells
SD2	Spinning stage day 2	The larval midgut epithelium detaches from the pupal epithelium. Active formation of the new pupal epithelium
PP	Prepupal stage	The larval midgut epithelium is shed into the lumen (yellow body). The new pupal epithelium continues to grow and differentiate
PD1-PD7	Pupal stage day 1 - day 7	Yellow body is actively digested. The new pupal epithelium differentiates into the adult midgut

Light microscopy (LM) and transmission electron microscopy (TEM)

Animals were quickly anestethized with CO_2 before dissection. They were cut dorsally, the midgut was immediately isolated and fixed in 4% glutaraldehyde (in 0.1 M Na-

cacodylate buffer, pH 7.2) overnight at 4°C. Specimens were then postfixed in 1% osmium tetroxide for 1 h, dehydrated in an ethanol series, and embedded in an Epon/Araldite 812 mixture. Semithin sections were stained with crystal violet and basic fuchsin and observed by using an Olympus BH2 microscope (Olympus, Tokyo, Japan). Images were acquired with a DS-5M-L1 digital camera system (Nikon, Tokyo, Japan). Thin sections were stained using uranyl acetate and lead citrate and observed by using a Jeol JEM-1010 electron microscope (Jeol, Tokyo, Japan) and images were acquired with an Olympus Morada digital camera.

To give a strong contrast to autophagosome membranes at TEM, after fixation in 4% glutaraldehyde, midguts were postfixed for 30 min in a solution of 2% osmium tetroxide in 0.1 M imidazole buffer at room temperature (Yla-Anttila et al., 2009), dehydrated in an ethanol series and embedded in Epon resin. Thin sections were observed by using a Jeol JEM-1010 electron microscope.

Scanning Electron Microscopy (SEM)

Midgut sections about 1-2 mm thick or yellow body cells extracted from pupal midguts at different developmental stages were fixed with 1% glutaraldehyde in 0.1 M Na-cacodylate buffer (pH 7.2) at room temperature (for 15 min yellow body cells and for 1 h midgut sections) and then three times washed in 0.1 M cacodylate buffer (pH 7.2). They were postfixed in a solution of 1% osmium tetroxide and 1,25% potassium ferrocyanide for 1 h 30 min at room temperature. Yellow body samples were embedded in polyfreeze cryostat embedding medium (Polyscience Europe, Eppelheim, Germany), stored at -20°C and immediately ready to be cut; the specimen was cut into sections about 8-10 µm thick that were collected on polylysinated slides. Cryosections and midgut sections were washed in phosphate buffered saline (PBS) (pH 7.2) and postfixed in the same solution of 1% osmium tetroxide and 1,25% potassium ferrocyanide for 30 min. Both samples were washed in phosphate buffered saline (PBS) (pH 7.2) and then immersed in 0.1% osmium tetroxide in PBS for 48 h (osmic maceration to remove cytosol, thus improving the visualization of cytoplasmic ultrastructure). Slices were dehydrated in an increasing series of ethanol, subjected to critical point drying with CO_2. Dried slices were mounted on stubs, gold coated with a

Sputter K250 coater, and then observed with a SEM-FEG XL-30 microscope (Philips, Eindhoven, The Netherlands).

Preparation of samples for immunohistochemistry and enzymatic histochemistry

For paraffin embedding the midgut was excised from the animal and fixed in 4% paraphormaldehyde in 0.1 M phosphate-buffered saline (PBS, pH 7.2) for 3 h at room temperature. Specimens were dehydrated in an ethanol series and embedded in paraffin. Sections (8-10 µm thick) were cut with a Jung Multicut 2045 microtome (Leica)) and used for immunostainings. Reference sections were stained with Mayer's hematoxylin (2% aqueous solution) and eosin (1% aqueous solution).

In order to prepare cryosections, midgut samples were immediately isolated after dissection, embedded in polyfreeze cryostat embedding medium (Polyscience Europe, Eppelheim, Germany), and stored in liquid nitrogen until use. Cryosections (8 µm thick) were obtained on a Leica CM 1850, and slides were immediately used or stored at -20°C. Reference sections were stained with a solution of DAPI (Sigma, Italia) diluted 1:5000 in phosphate buffered saline 1M (PBS) (pH 7.2) to evidence nuclei.

Histochemistry

a. *Periodic acid-Schiff*

Paraffin sections were deparaffinised by treatment with Bioclear, rehydrated in an ethanol series, and then processed for Periodic acid-Schiff (PAS) staining (Bio-Optica Histopathological kit, Bio-Optica) according to manufacturer's instructions to evidence the presence of glycogen (Pearse, 1960).

b. *NADH-diaphorase*

To localize NADH-diaphorase (EC 1.9.3.1) activity associated to mitochondria in midgut tissues (Pearse, 1960), cryosections were rehydrated and then processed with the Histopatological kit (Bio-Optica, Milano, Italy) according to the manufacturer's instructions.

c. *Acid phosphatase*

To localize acid phosphatase (EC 3.1.3.2) activity, cryosections were rinsed with PBS for 5 min and subsequently incubated in a 0.1N sodium acetate-acetic acid buffer pH

5.0-5.2 (25 °C), containing 0.01% naphthol phosphate AS-BI (Sigma-Aldrich, St. Louis, USA), 2% *N′-N′*-dimethylformamide, 0.06% fast red violet LB (Sigma-Aldrich) and 0.5mM $MnCl_2$. Incubations were performed for 90 min at 37°C. For ultrastructural localization of acid phosphatase, midguts were fixed in Karnovsky's fixative for 2 h at 4°C. After a rinse in 40 mM Tris/maleate buffer pH 5.2, samples were incubated in the same buffer containing 8 mM sodium β-glycerophosphate and 2.4 mM lead nitrate for up to 2 h at 37°C. The tissue was post-fixed with 1% osmium tetroxide for 1 h and processed for Epon embedding as described in the "Light microscopy and transmission electron microscopy".

Analysis of membrane integrity in yellow body cells

Yellow body cells were extracted from pupal midguts and washed by centrifugation in a sterile Saline Solution for Lepidoptera (SSL) (210 mM Sucrose, 45 mM KCl, 10 mM Tris-HCl, pH 7.0). They were mounted on concavity slides (Carolina Biological Supply, Burlington, USA) to avoid damage during processing and incubated in 100 μl SSL containing 10 μM Ho33258 and 10 μM propidium iodide (PI) for 10 min at room temperature (Tettamanti and Malagoli, 2008). Coverslips were mounted with Citifluor (Citifluor, London, UK) and samples were immediately observed using the following Ex/Em wavelengths: 343/483 nm (Ho33258) and 536/617 nm (PI). Since PI is unable to cross intact membranes, only cells that showed double labeling were characterized by plasma membrane damage (Dartsch et al., 2002).

Expression of BmAtg8 protein and antibody preparation

pET-28b-*BmATG8* expression vector, provided by Professor Congzhao Zhou (University of Science and Technology of China) (Hu et al., 2010), was used to transform *E. coli* Rosetta cells. The expressed recombinant protein (approximate molecular weight 14 kDa, (Hu et al., 2010)) was purified using Ni-NTA columns (GE Co., Uppsala, Sweden) and the purity of the protein was checked by 15% SDS-PAGE. The His-tag purified protein was further purified using a Sephadex G-10 column (Pharmacia, Piscataway, USA) and checked using 15% Tricine-SDS-PAGE.

The purified protein was used to immunize New Zealand white rabbits (Sambrook et al., 1989). Three injections were made in the abdomen of the rabbits with 1.2, 0.6

and 0.3 mg protein, respectively. Afterwards, the antiserum was collected and affinity-purified and the antibody titer was measured using the ELISA method (GenScript Co. Ltd, Nanjing, China).

Immunohistochemistry

Phospho-Histone H3 (H3P) antibody

After deparafinization the sections were treated with 3% H_2O_2 to inhibit endogenous peroxidases. Sections were incubated for 30 min with a solution of 2% BSA, 0.1% Tween 20 in PBS and then for two hours at room temperature with an anti-H3P antibody (Catalog no. 06-570) (Upstate, Newyork, USA), at a diluition of 1:100. Incubation with an appropriate HRP-conjugated secondary antibody (diluted 1:100) was performed for 1 h at room temperature. A DAB substrate was used to detect the HRP-conjugated secondary antibody. Antibodies were omitted in control samples.

BmAtg8

Paraffin sections were dewaxed using xylene and rehydrated in an ethanol series. Anti-BmAtg8 antibody (1 µg/µl) was labeled with fluorescein isothiocyanate (FITC) at 1:5 dilution according to the method of Cardoso et al. (2008). Sections were incubated with BmAtg8-FITC conjugated antibody (diluted 1:100 in 1% BSA) for 1 h at 37 °C. Sections were examined under a Laser Scanning Confocal Microscope (LSM 510 META DUO Scan, Carl Zeiss Co., Germany). Reference sections were stained with hematoxylin and eosin under a light microscope.

Cleaved caspase-3

After deparaffinization the sections were subjected to an antigen unmasking procedure by heating in 10 mM sodium citrate buffer (pH 6.0) for 5 min and then allowing them to cool. They were then treated with 3% H_2O_2 for 10 min to inhibit endogenous peroxidases. Sections were incubated for 30 min with a solution of 2% BSA, 0.1% Tween 20 in PBS and then overnight at 4°C with an anti-cleaved caspase-3 antibody (catalog no. 9661) (Cell Signaling Technology, Beverly, USA), at a dilution of 1:100. Incubation with an appropriate HRP-conjugated secondary antibody (diluted 1:50) was performed for 1 h. A DAB substrate was used to detect the HRP-conjugated secondary antibody. Antibodies were omitted in control samples.

Western blot analysis

BmAtg8

Total proteins were extracted from larval and pupal midguts using a protein extraction solution (Beyotime Co., Shanghai, China). SDS-PAGE was conducted, loading 10 μg protein per lane. After electrophoresis, proteins were transferred to polyvinylidene fluoride (PVDF) membranes (Beyotime). The membranes were saturated with 5% milk and then were blotted with anti-BmAtg8 antibody at a dilution of 1:800 overnight at 4 °C. After three washings, the membranes were blotted with a horseradish peroxidase (HRP)-labeled sheep anti-rabbit IgG (Beyotime) at a dilution of 1:1000. The reactivity of the antibody on the membranes was revealed by using a SuperEnhanced Chemiluminescence Detection Kit (Applygen Technologies Inc., Beijing, China).

Cleaved caspase-3

Total proteins were extracted as follows. Midguts were homogenized in a glass-Teflon Potter homogenizer in 1 ml/0.1 g tissue of a buffer solution (100 mM mannitol, 10 mM HEPES-Tris at pH 7.2, 1× protease inhibitor cocktail, Sigma-Aldrich). Homogenates were clarified by centrifugation (15000×g for 15 min at 4°C). Proteins were denatured by boiling the samples in 2× gel loading buffer. SDS-PAGE was performed on AnykD Mini-PROTEAN TGX Gels (BioRad, Hercules, USA) by loading 45 μg protein per lane. After electrophoresis, the proteins were transferred to nitrocellulose membranes (Thermo Fisher Scientific, Rockford, USA). Membranes were saturated with a solution of 3% milk in TBS and 0.1% Tween 20 in TBS overnight at 4°C and subsequently incubated with an anti-rabbit cleaved caspase-3 polyclonal antibody (catalog no. 9661) (Cell Signaling Technology) at a dilution of 1:500 for 2 h at room temperature. Antigens were revealed with an appropriate HRP-conjugated secondary antibody (diluted 1:5000, Jackson Immuno Research Laboratory, West Grove, USA). Immunoreactivity was detected with SuperSignal West Femto Substrate (Thermo Fisher Scientific). Since the use of “housekeeping proteins” as internal standards may be unsuitable due to variations in protein concentration of control proteins among samples, the influence of physiological and pathological factors on their expression, defects in blot transfer and protein underestimation (Ferguson et al., 2005; Romero-Calvo et al., 2010; Welinder and Ekblad, 2011), we adopted a

Coomassie staining procedure (Welinder and Ekblad, 2011) to assess equal gel loading and blotting efficiency.

Acid phosphatase activity assay

Midguts were dissected on ice and, after a rinse in SSL, were stored in liquid nitrogen until use. After being thawed, midguts were homogenized (nine strokes at 2000 rpm in a glass-Teflon Potter homogenizer) in 1 ml/0.1 g tissue of the following homogenization buffer: 100 mM mannitol, 10 mM HEPES-Tris at pH 7.2. A protease inhibitor cocktail (Sigma-Aldrich) was added during the homogenization procedure. The protein concentration in the homogenates was determined according to Bradford assay (Bradford, 1976), with BSA as a standard. The enzyme activity in the homogenates was assayed with 4-nitrophenyl phosphate as a substrate at a fixed incubation time of 30 min, according to the method reported by Moss (1983). The reaction was performed at 25°C and stopped by adding 4 ml of 0.1 M sodium hydroxide. Colour development was determined at 405 nm using an Ultrospec 3000 spectrophotometer (Amersham Pharmacia Biotech, Milano, Italy). Each value was the result of at least six experiments performed on midgut samples from three series of animals.

Evaluation of ATP content

Homogenates from midguts were prepared as described in the "Acid phosphatase activity assay" section. Homogenates were clarified by centrifugation (15000×g for 15 min at 4°C). Protein concentration was determined by using a BCA Protein Assay Kit (Thermo Fisher Scientific), taking BSA as a standard, and adjusted to 1 mg/ml with homogenization buffer. ATP levels were quantified by using the ATP Bioluminescence Assay Kit (Roche, Mannheim, Germany), following the manufacturer's instructions. Briefly, 25 µg cytosolic protein and an equal volume of reagents were added to a white-walled, 96-well plate and the light signal was immediately read with a Tecan microplate reader Infinite F200 (Tecan Group, Männedorf, Switzerland). Each experiment was performed at least in triplicate on midgut samples from three series of animals.

Measurement of caspase activity

Homogenates from midguts were prepared as described in the "Acid phosphatase activity assay" section. Homogenates were clarified by centrifugation (15000×*g* for 15 min at 4°C) and protein concentration was adjusted to 1 mg/ml with homogenization buffer before storage at -80°C. Caspase activity was determined (at least in triplicates on midgut samples from three series of animals) by using a Caspase-Glo 3/7 kit (Promega, Madison, USA) as follows: 10 µg cytosolic protein and an equal volume of reagents were added to a white-walled, 96-well plate and incubated at room temperature for 1 h. The luminescence of each sample was measured in a Tecan microplate reader Infinite F200.

TUNEL assay

Paraffin sections of midgut samples were prepared as described above for caspase-3 immunohistochemistry. DNA fragmentation in apoptotic cells was identified by using the DeadEnd Colorimetric TUNEL System (Promega). Briefly, paraffin sections were deparaffinized, rehydrated through graded ethanol washes, and rinsed with PBS. Proteinase K (20 µg/ml) digestion was applied as a pre-treatment for 20 min at room temperature. Incubation with the rTdT reaction mix was performed for 1 h at 37°C, in accordance with the instructions provided by the manufacturer. The reaction was terminated by immersing the slides in 2× standard sodium citrate (15 min). A pre-treatment with 3% H_2O_2 (5 min) preceded the incubation with a streptavidin-HRP solution (diluted 1:500 in PBS, 30 min). A DAB solution was used for signal development. Sections were counterstained with hematoxylin and eosin. Negative controls were performed by replacing rTdT enzyme with water in the rTdT reaction mix.

Quantitative real-time PCR (qRT-PCR)

RNA was isolated using Trizol Reagent (Invitrogen Co., Carlsbad, USA) according to the manufacturer's instructions and emplyed to synthesize the first chain of cDNA by the cDNA Synthesis Kit (TOYOBO Co., Osaka, Japan). Primers for quantitative real-time PCR (qRT-PCR) were designed according to the sequences of the target genes (Table 2). In detail, we evaluated the expression of autophagy-related genes *BmATG5*

(GenBank accession number NM_001142487), *BmATG6* (NM_001142490) and *BmATG8* (NM_001046779) (Zhang et al., 2009; Mizushima et al., 2010), and apoptosis-related genes *BmICE-2* (DQ360829), *BmCaspase-4* (HQ456874) and *BmIAP* (NM_001043559) (Zhang et al., 2010; Courtiade et al., 2011). *BmActinA3* gene (NM_001126254) was used as a control (Zhang et al., 2009; Li et al., 2010). qRT-PCR was performed according to SYBR-GREEN1 fluorescent relative quantitative approach (Livak and Schmittgen, 2001), using ABI7300 fluorescence quantitative PCR system (Applied Biosystems, Carlsbad, USA). Three independent duplicates were conducted for each of the data sets. Relative gene expression ($2^{-\Delta\Delta CtA,B}$) was calculated according to the equation of $2^{-\Delta CT}$, where ΔCT equals the difference between the CT values of the target genes and *BmActinA3* gene according to the manufacturer's instructions.

Table 2. Primer sequences used for the amplification of apoptosis- and autophagy-related genes

Gene	Forward primer sequence	Reverse primer sequence
BmATG5	CCAAACAAAGATGTAGTAGAAGCA	GTCTGTTGATAGCCCAAAACTG
BmATG6	AACTGTATTGCTCCTCTCTTCG	GCGACCATTGCCGCATCG
BmATG8	AGAAGAACATTCATTTGAGAAGAGA	AATCAGACGGAACTAAATACTTC
BmICE-2	GGCGATAGCGGCGAAGTA	ATGCGTTGGAAGGCGTAA
BmCaspase-4	CTGTTGAAAGCGTGTTTG	AATTCGTATGTCGTAGCG
BmIAP	GGTGAAAGGACGTGACTACAT	CGCTCCTCGGAATAACATA
BmActinA3	CGGGAAATCGTTCGTGA	ACGAGGGTTGGAAGAGGG

RESULTS

Morphological changes of the alimentary canal and midgut degeneration during larval-pupal metamorphosis

During the fifth larval instar (Figs. 1A, B), the alimentary canal of larvae was a long and thin tube. The midgut had a turgid aspect, attributable to the presence of food in the lumen, and represented the main part of the digestive system; it was also covered by ramified tracheae. However, at wandering stage (Figs. 1C, D), cessation of feeding occurred: this event was followed by a purge of the alimentary canal. Midgut changed from light brown to colorless and progressively decreased in diameter. During the terminal part of the spinning phase (Figs. 1E, F), the gut became progressively shorter and thinner, with folds on the outer surface of the midgut region (Fig. 1F), and acquired a dark red colour due to the formation of the yellow body in the lumen. At pupal stage (Figs. 1G-J), the midgut dramatically changed its form; the midgut was characterized by a thin wall and by a strongly stained inner content composed by the yellow body in degeneration. After adult eclosion (Figs. 1K, L), a conical and dark-colored midgut was visible.

Light microscopy observations revealed that the midgut tissue both degenerated and regenerated during metamorphosis. At the fifth larval instar the midgut epithelium was formed by columnar and goblet cells (Fig. 2A). Columnar cells were numerous and characterized by a thick brush border toward the lumen, whereas goblet cells showed a basal nucleus and a goblet-shaped cavity, lined by tightly arranged microvilli (Fig. 2B). Nuclei of larval epithelial cells showed uncondensed chromatin (Fig. 2C). The cytoplasm of columnar cells was characterized by the presence of abundant rough endoplasmic reticulum and mitochondria (Fig. 2D). Along the whole epithelial surface high exocytotic activity was visible (Fig. 2E, F). Sparse stem cells were visible in the basal region of the epithelium, which is encircled by a thin extra-epithelial layer, composed of muscles fibers and tracheae (Fig. 2A).

At wandering stage, stem cell proliferation initiated (Fig. 2G), as demonstrated by positivity for H3P (Fig. 2H) visible in the basal region of the midgut epithelium.

The proliferation and differentiation of stem cells led to the formation of a continuous cell layer (the future pupal epithelium) that began to push the larval midgut

epithelium toward the lumen (Figs. 3A-C). A concurrent degeneration of larval midgut could be observed since the spinning stage. At this stage the larval midgut epithelium detached from the new pupal epithelium (Fig. 3C): columnar and goblet cells lost their morphology, although their brush border remained intact (Fig. 3D).

Stem cells undergoing differentiation were characterized by a large inner compartment covered by short cytoplasmic projections (Figs. 3D, E); these projections became shorter and thinner (Fig. 3F) during differentiation process.

At prepupal phase (Fig. 4A) a new cell layer formed by stem cells was observable. The new epithelium was remodelled during larval-adult transformation leading to the formation of a well organized pupal epithelium (Fig. 4B), where microvilli completely covered the whole apical surface (Fig. 4C) and the integrity was ensured by a junctional system (Fig. 4D).

The cytoplasm of the new epithelial cells contained a great amount of fat droplets surrounded by glycogen granules (Figs. 4E, F), as well as round vesicles of various sizes (Fig. 4G), which were exocytosed throughout the pupal period (Figs. 4C, H). Their cytoplasm contained also spherites (Figs. 4H, J), that are structures involved in the degeneration of Ca^{2+} ions (Waku and Sumimoto, 1971). There was no evidence of the large inner compartment seen during the spinning phase (Fig. 3D).

At late stage of degeneration, the larval epithelium gave rise to a compact mass of cells in the lumen, called yellow body, that was progressively digested (Figs. 4A, B). These cells modified their shape (Fig. 5A): columnar and goblet cells progressively shrank and underwent ruptures (Fig. 5B), and their organization completely changed, although at early stages of tissue degeneration contacts among cells were still observable (Fig. 5C). Nuclei of these cells showed condensed chromatin (Figs. 5D, E).

Pupal midgut was remodelled until the end of pupal phase to form the midgut epithelium typical of the adult (Figs. 6A-C). This epithelium was thin and exhibited a well-organized brush border, with microvilli more seldom and flattened than in the larval and pupal one (Fig. 6B), and it was characterized by abundant endoplasmic reticulum and mitochondria (Fig. 6B). The presence of few, small isolated cells in the basal region of the epithelium was observed (Figs. 6C, D), while the apical portion of adult epithelium cells contained many granules and vesicles that were exocytosed in the midgut lumen (Figs. 6E, F).

These observations indicated that the growth of a new pupal epithelium was concomitant with the degeneration of the old larval midgut, that started prior to pupation, became most active in early pupae and lasted up to adult eclosion (Table 1).

Histochemical characterization of larval and pupal midgut

a. *PAS* (glycogen detection). During fifth instar, glycogen granules were present in the cytoplasm of larval cells (Figs. 7A, B), whereas after the formation of the new pupal midgut positivity was mainly localized in the new epithelial layer (Figs. 7C-F). Glycogen content progressively decreased in larval midgut cells and no reactivity was detectable inside the yellow body (Figs. 7E, G).

b. *NADH-TR reactivity* (marker for mithocondrial activity). During larval period, staining was detectable in the whole epithelium (Figs. 8A, B). A progressive reduction of metabolic activity was evident in degenerating columnar and goblet cells that were disgregating until their complete demise within the yellow body (Figs. 8C-H). Since the first day of spinning high mitochondrial activity was visible in the whole pupal midgut epithelium (Figs. 8C-E). When the new pupal epithelium was well-developed, NADH staining was resumed in the basal and apical regions of the cells (Figs. 8F, H). The reactivity was maintained in the adult midgut (Figs. 8I, J).

Morphological features of autophagy

To determine whether autophagy is involved in the degeneration of *B. mori* larval midgut, we examined morphological features attributable to this mechanism. Starting from spinning stage, autophagic compartments were clearly observed in the larval midgut cells and they were highly represented until early pupation (Figs. 9A-E). The presence of a double-limiting membrane was the hallmark of autophagosomes (Figs. 9A, C). Autolysosomes, surrounded by lysosomes (Figs. 9B, D), contained digested cellular material and organelles at different stages of degeneration (Fig. 9B). In addition, myelin-like figures, which represent the result of autophagic degradation of membranous cellular components (Martinet and De Meyer, 2008), were visible in larval midgut cells (Fig. 9E).

mRNA expression of autophagy-related genes

Molecular markers that are associated with autophagy were evaluated to assess the onset of the autophagic pathway in midgut during metamorphosis. To this aim three autophagy-related genes, *BmATG5*, *BmATG6* and *BmATG8*, were examined. These genes encode proteins that are involved in early stages of autophagosome biogenesis, i.e autophagosome nucleation and expansion; therefore they are good markers of the activation of the autophagic program. qRT-PCR analysis indicated that these genes were expressed at various degrees in the midgut during larval-pupal transformation (Figs. 10A-C). In detail, high levels of expression of all these genes were detected at the wandering stage, before morphological features of autophagy appeared (Fig. 9). During the spinning period and in pupae, the expression levels of these genes decreased to a more or less constant level. It is worthy to note that the expression of *BmATG5* showed a second peak during the prepupal stage (Fig. 10A).

Expression and localization of the autophagy-related protein BmAtg8

To confirm gene expression results, we analyzed the expression and processing of Atg8 protein, a factor involved in the expansion of the isolation membrane that leads to autophagosome formation (Mizushima et al., 2010). To this end, we performed western blot analysis with anti-BmAtg8 antibody on protein extracts from midguts of larvae at wandering, spinning and prepupal stages, and of pupae at 24 h (PD1) and 48 h (PD2) post pupation (Fig. 11A). A 14 kDa band corresponding to BmAtg8 protein, and a band related to phosphatidylethanolamine-conjugated form of BmAtg8 protein (BmAtg8-PE), a marker associated with completed autophagosomes (Klionsky et al., 2008), were detected at wandering stage. Their expression was maintained up to early pupal stage (Fig. 11A).

Timing and localization of BmAtg8 protein in midgut tissues were assessed by immunohistochemical analysis using FITC-labeled anti-BmAtg8 antibody on midgut samples from animals at different stage of development (Figs. 11B-J). During wandering stage (Figs. 11B, E, H), BmAtg8 protein was localized in larval midgut cells undergoing degeneration. Positivity for BmAtg8 antibody was also found in spinning (Figs. 11C, F, I) and pupal samples (Figs. 11D, G, J). In these animals, the

fluorescent signal was always restricted to the cells of the yellowbody, while it was absent in the new pupal mifgut epithelium (Figs. 11F, G, I, J).

Analysis of acid phosphatase

Formation of autolysosomes requires the recruitment of lysosomes and their fusion to autophagosomes. For this reason we evaluated lysosomal activity during larval midgut degeneration by monitoring acid phosphatase. A specific spectrophotometric assay was used to accurately quantify the activity of this enzyme in midgut cells during the period of larval-pupal transformation. The enzymatic activity increased considerably during the spinning period, reaching a peak during spinning (SD2), when high autophagic activity could be detected; after enzymatic activity decreased, moderate activity was resumed in pupal midguts (Fig. 12A). By histochemical staining we were able to evaluate the distribution of acid phosphatase activity in midgut tissues. During the fifth larval instar, only little activity was present in the apical region of midgut cells (Fig. 12B). The intensity of the signal increased during spinning stage (Fig. 12C). Afterwards, acid phosphatase activity was also found in pupal samples (Fig. 12D). The enzyme activity was always restricted to the cells of the larval midgut epithelium during degeneration, whereas it was absent in the new pupal midgut epithelium (Figs. 12C, D). Ultrastructural analysis confirmed this staining pattern and demonstrated that acid phosphatase activity was localized in numerous cytoplasm dots in degenerating cells (Figs. 12E, F). These corpuscles apparently corresponded to autolysosomes, as indicated by compartments in which acid phosphatase staining and degenerated cellular structures coexisted (Figs. 12F, G).

Morphological features of apoptosis

In eukaryotes, apoptosis is characterized by specific features, such as nuclear chromatin condensation and DNA fragmentation (Kerr et al., 1972). Both features were found in larval midgut from early pupae. Evidence of nuclear pyknosis (Figs. 13A, B), as well as nuclear fragmentation (Figs. 13C, D), was observable in these cells. Following condensation, chromatin acquired a very compact aspect (Fig. 13B) that greatly differed from the physiological chromatin distribution observed in nuclei of midgut cells of larvae at feeding stage (Fig. 13E).

Expression of apoptosis-related genes

The expression of two caspase genes, *BmICE2* and *BmCaspase-4*, and that of *BmIAP*, an inhibitor factor that contributes to keeping caspases in insects, was analyzed by qRT-PCR to determine the timing of apoptosis-related genes expression in the midgut during metamorphosis. The results indicated that *BmICE-2* and *BmCaspase-4* were highly expressed at the end of the fifth larval instar. After that peak, their expression decreased and, during pupal stage, levels of expression were low for both genes (Figs. 14A, B). *BmIAP* was highly expressed during the last day of the fifth larval instar and wandering stage, while its expression decreased at spinning stage (Fig. 14C).

Analysis of activated caspases

To assess the occurrence of activated caspases during the remodeling of larval midgut epithelium, immunostaining experiments were performed (Figs. 15A-H) by using an antibody able to detect cleaved caspase-3 which has been previously used in *Drosophila melanogaster* (Griswold et al., 2008), *B. mori* (Goncu and Parlak, 2011) and other Lepidoptera (Parthasarathy and Palli, 2007b; Tettamanti et al., 2007a; Vilaplana et al., 2007). While no positivity was found in the midgut epithelium during the fifth larval instar (Figs. 15A, B), the antibody recognized several midgut cells of spinning larvae (Figs. 15C, D) and pupae (Figs. 15E, F). The immunopositivity was visible only in larval midgut cells, while no signal could be detected in the new pupal epithelium (Fig. 15F). Immunoblot analysis carried out on midgut samples from animals at different stage of development validated the previous assay and demonstrated that the antibody reacted specifically with *B. mori* activated caspase-3 (Fig. 15I). A strong 15 kDa band was visible at spinning phase (SD2) and, after decreasing in prepupal midguts, high levels of the protein were detected from the first day of pupation (Fig. 15I). Measuring of the activity of effector caspases by using a specific DEVD substrate confirmed the immunoblot results. In fact, the activity peaked at late spinning stage (SD2) and, after a fall, it progressively rose again from PD1 onwards (Fig. 15J).

Analysis of DNA fragmentation

TUNEL assay was performed to evaluate the specific localization of nuclei undergoing DNA fragmentation in midgut tissues (Figs. 16A-H). During the fifth instar no nuclei in the midgut cells were stained (Figs. 16A, B), while positivity was assessed in some cells of the larval midgut starting from the spinning phase (Figs. 16C, D). The number of positive cells increased massively within the yellow body of day 2 pupae (Figs. 16E, F). Positivity was never detected in the newly formed pupal epithelium (Figs. 16C, E).

Evaluation of membrane integrity

The Ho33258-PI fluorescent staining, performed on yellow body cells undergoing degeneration, showed that the plasma membrane of some, but not all, cells within the yellow body was permeable to both Ho33258 and PI (Figs. 17A, B); in contrast, cells with a normal nucleus, and thus still viable, were not stained by PI (Figs. 17A, B). The membrane damage in some cells of the yellow body was confirmed by TEM observations (Fig. 17C).

Evaluation of protein concentration and mitochondrial activity

Generally, when cells are deprived of nutrients, they set autophagy to break down part of their content, generating molecules and energy to survive. To investigate whether autophagy has a pro-survival role in midgut during metamorphosis, we analyzed three parameters that are related to the metabolic activity of the cell, i.e. protein content, mitochondrial activity and ATP production, in midgut samples from late fifth larval instar up to early pupae. In fact, autophagy peaked in this window, while apoptosis was still beginning (Figs. 9-16).

Initiation of wandering resulted in a reduction of protein concentration in midgut cells, which continued during the whole spinning period. The amount of proteins started to raise at prepupal phase (Fig. 18A). Measurement of ATP revealed a 30-fold increase, compared to wandering stage, in ATP levels in larval midguts since SD1, which continued to grow heavily until prepupal phase (Fig. 18B). A strong staining for NADH-TR in the midgut epithelium demonstrated the occurrence of high mitochondrial activity in these cells at the beginning of spinning phase (SD1) (Figs. 8C-E), when the massive increase of ATP levels was detected (Fig. 18B).

DISCUSSION

Replacement of silkworm midgut during fifth larval instar

Histolysis of larval organs is one of the key events that occurs in holometabolous insects: this entails the growth and differentiation of adult structures together with the destruction of old cells (Baehrecke, 1996). The organs affected by tissue rearrangement include salivary glands, fat body, motoneurons, and the alimentary canal (for a review, see Yin and Thummel, 2005). In particular, massive gut remodelling occurs in response to the need for the provision of nutrients during the pupal period and for the renewal of an organ that has to fulfill adult alimentary requirements (Wigglesworth, 1972; Dow, 1986).

The present work shows that the midgut is completely replaced in *Bombyx mori* larvae during fifth larval instar, forming a new functional midgut that is maintained during the pupal period and is remodelled to form the gut in the adult.

The replacement of silkworm midgut is carried out through a series of events that leads to the disappearance of the old epithelium and the formation of a new epithelium.

At the beginning of the fifth larval instar, when the larva feeds and rapidly grows, the midgut is a functional organ characterized by metabolically active columnar cells, which are full of mitochondria, show a positivity for NADH-TR, and are characterized by a well-developed brush border. Goblet cells, important for the ionic regulation of the gut (Wieczorek et al., 2000), have a normal shape with well-organized microvilli. The presence of fat droplets and glycogen content in the cytoplasm of these cells is related to their high metabolic activity. This accumulation of glycogen and lipids and mitochondrial activity progressively disappear in yellow body cells since the spinning stage, consistent with the degeneration of these cells and the occurrence of cell death processes.

The abundant presence of autophagic vacuoles in the yellow body, as well as the decreasing content of glycogen and lipids in yellow body cells at pupal stage suggest a mobilization of nutrients from these larval cells. This evidence is consistent with the features observed in the newly formed midgut tissue. In fact, the pupal epithelium accumulates glycogen and lipid droplets, displays metabolic activity, is characterized

by an apical brush border and shows intense exocytosis activity. All these characteristics indicate that the new midgut epithelium is functional and performs digestive processes, at least during the early period of adulthood, and that molecules derived from the degenerating larval epithelium could work as food substrates (Tettamanti et al., 2007a).

The accumulation of considerable amounts of glycogen and lipids within midgut cells has been previously reported (de Eguileor et al., 2001; Uwo et al., 2002), but the role of storage molecules in *B. mori* pupal midgut cells is not yet clear. Indeed, they might represent an additional energy source during pupal-adult development after degeneration of the fat body (Larsen, 1976; Iwanaga et al., 2000).

Although differentiation of stem cells into diverse adult cell types has been described in several holometabolous insects such as *Heliothis virescens* (Tettamanti et al., 2007a), *Manduca sexta* (Hakim et al., 2010) and *Drosophila melanogaster* (Micchelli and Perrimon, 2006; Ohlstein and Spradling, 2006), here we show that, at the larval-pupal transition, these cells differentiate into a unique cell type similar to columnar cells. The lack of differentiation of stem cells into goblet cells during this last molt, as happens *in vivo* during the larval-larval molts (Baldwin and Hakim, 1991) and *in vitro* in stem cell cultures (Sadrud-Din et al., 1996), is in agreement with an adaptation of the new midgut physiological properties to the nutritional requirements of the moth, which feed on nectar (Dow, 1986; Baldwin et al., 1996), or which does not feed as it occurs in *B. mori* adult.

The involvement of stem cells in replacing the larval midgut has been described in insect larvae of various orders in which this process shows variations in relation to timing, the number of cells involved, and their differentiation fate (Baldwin and Hakim, 1991; Jiang et al., 1997; Martins et al., 2006). In particular, the sequence of events described here about the complete replacement of larval midgut before pupation is similar to that reported for *Galleria mellonella* (Uwo et al., 2002) and *H. virescens* (Tettamanti et al., 2007a).

It is noteworthy that stem cell proliferation and differentiation act more quickly than in *H. virescens*. On the other hand, histological and molecular data about the occurrence of degeneration in the yellow body cells demonstrate that the degradation

of the larval midgut is a gradual process and this takes place more slowly than what happens in *H. virescens*.

Of note, in accordance with descriptions for *M. sexta* (Russel and Dunn, 1991; Baldwin et al., 1996), *B. mori* (Waku and Sumimoto, 1971), and *H. virescens* (Tettamanti et al., 2007a), in silkworm stem cells undergoing differentiation are characterized by the presence of a large amount of vesicles that contain electron-dense material which is secreted into the lumen. As suggested by Waku and Sumimoto (1971) these vacuoles may contain lysozyme.

Although in the midgut of adult butterflies and moths stem cells have not been described yet, the presence of small isolated cell nests that we observed in the basal region of the epithelium need to be carefully investigated, to ascertain the true nature of these cells.

Midgut remodelling and cell death processes

Previous work has described the occurrence of apoptosis in larval organs of Lepidoptera during metamorphosis (Dai and Gilbert, 1997; Uwo et al., 2002; Mpakou et al., 2006; Parthasarathy and Palli, 2007b; Tettamanti et al., 2007a; Vilaplana et al., 2007; Sumithra et al., 2010), while robust biochemical and molecular evidence for the involvement of autophagy is still lacking (see Malagoli et al., 2010 for review). In addition, the role of autophagy, as well as its relationships with apoptosis, are troublesome and still under debate (Malagoli et al., 2010; Tettamanti et al., 2011). Indeed there is much confusion regarding acceptable methods for monitoring autophagy in higher eukaryotes (Klionsky et al., 2008) and cell death mechanisms taking place in organs and tissues of Lepidoptera appear to have somehow peculiar features.

With the aim to overcome this fragmentation of knowledge, we performed a detailed morphological, cellular, biochemical and molecular analysis of the remodeling process that occurs in the larval midgut of *B. mori* during metamorphosis.

Our study demonstrates the occurrence of both apoptotic and autophagic events in the desappearance of the larval midgut epithelium, as discussed below.

Involvement of autophagy in *B. mori* midgut remodeling

Several lines of evidence from the present study clearly demonstrate that autophagy occurs in the midgut of *B. mori* and is actively involved in the remodeling of this organ during larval-pupal transformation: i) presence of morphological autophagic features in larval midgut cells; ii) expression of autophagy-related genes in larval midgut cells; iii) localization of BmAtg8 in larval midgut cells, as well as its processing to BmAtg8-PE, a key protein marker that is reliably associated with completed autophagosomes (Klionsky et al., 2008): only a few descriptions of Atg8 processing through western blot analysis in invertebrates have been published, especially among insects (Buzgariu et al., 2008; Shelly et al., 2009; Barth et al., 2011; Chiarelli et al., 2011), and to our knowledge this is the first report of such an effective Atg8 antibody developed for Lepidoptera; iv) increased activity and expression of acid phosphatase, a lysosomal marker that is used to follow autophagy (Klionsky et al., 2008), in cytoplasmic granules and putative autolysosomes that are present in degenerating midgut cells.

Denton et al. (2009) demonstrated that autophagy, and not apoptosis, is essential for midgut cell death in *Drosophila* during metamorphosis. They found that combined mutants of the main initiator and effector caspases could not suppress midgut cell death, and inhibition of the caspase Decay, which is responsible for most of the caspase activity in dying midguts, has no effect on midgut removal. By contrast, midgut degradation is severely delayed in *ATG1*, *ATG2* and *ATG18* mutants (Denton et al., 2009, 2010). Although our data show that the autophagic process contributes to midgut demise in silkworm, the lack of a functional analysis for *BmATG* genes prevents us from assessing whether autophagy is essential for midgut cell death as in *Drosophila*. Nevertheless, we have provided evidence about its role in this remodeling process as discusses below.

Apoptosis and cell death

In addition to autophagy, we showed that also apoptosis occurs in silkworm midgut, in accordance with some previous studies (Parthasarathy and Palli, 2007b; Tettamanti et al., 2007a; Vilaplana et al., 2007). A peak in caspase transcription at the end of the fifth larval instar, and a decrease in *BmIAP* expression at early spinning, marks the

onset of the apoptotic signaling pathway. Transcription of caspase genes is followed by an increase in effector caspase activity in the larval epithelium from spinning stage. This delay could be due to the action of inhibitor of apoptosis protein (BmIAP), whose gene is highly expressed until wandering stage, which may inhibit the activation of caspases and therefore the apoptotic pathway until that time. Activation of the apoptotic pathway is consistent with the timing of the appearance of clear apoptotic features such as nuclear condensation and DNA fragmentation in the larval midgut cells (Dupere-Minier et al., 2004).

The larval midgut disappears gradually since death does not occur simultaneously in all cells. In fact, the loss of plasma membrane integrity occurs only in groups of yellow body cells at late stage of degeneration and not in the whole yellow body, as demonstrated by PI incorporation. This event is considered a point-of–no-return and is used as an indisputable marker of unavoidable cell death (Kroemer et al., 2009). The abundance of apoptotic features within these cells indicates that apoptosis is actually responsible for cell death during late pupal phase. In accordance with our hypothesis it must be underlined that apoptosis is usually involved in the removal of small groups of cells, while autophagic cell death leads to the simultaneous disappearance of large populations of cells (Thummel, 2001) as seen in our model, in which the whole larval midgut epithelium is removed.

Timing of appearance of autophagy and apoptosis

Although some studies have shown the concomitant presence of autophagic and apoptotic features in midgut of lepidopteran larvae (Tettamanti et al., 2007b; Vilaplana et al., 2007), no one has yet clearly demonstrated whether autophagy and apoptosis occur simultaneously or one takes place prior to the other. In silkworm midgut, autophagy occurs from wandering/spinning phase, as demonstrated by several specific markers. On the other hand, for apoptosis, a peak in caspase gene expression at the end of the fifth larval instar is followed by activation of effector caspases from spinning phase. Once caspases are activated, apoptosis is set in motion and features typical of this process can be found from prepupal/early pupal stage onward. These data demonstrate that autophagy is initiated earlier than apoptosis and apoptotic features appear after autophagic ones (Fig. 19). It seems

plausible that this pattern is linked to the ecdysone titer in the hemolymph (Rybczynski, 2005), with an autophagic burst at wandering/early spinning, followed by the onset of apoptosis at beginning of pupation, that drives cell demise.

Recently, interactions between autophagy and apoptosis pathways were reported (Eisenberg-Lerner et al., 2009) and some molecular mediators that regulate this cross-talk were described (Yue et al., 2003; Codogno and Meijer, 2006; Scott et al., 2007; Eisenberg-Lerner et al., 2009). In particular, Atg5 has been found to play important roles in the connection between the autophagic and the apoptotic pathway (Codogno and Meijer, 2006; Yousefi et al., 2006).

Future studies should be undertaken to resolve the role of *BmATG5*, whose mRNA has been shown to have a second peak of expression when apoptosis starts, which would give insight into a possible cross-regulation between autophagy and apoptosis in *B. mori* midgut cells.

Role of autophagy in silkworm midgut remodeling

In insects, autophagy fulfills multiple functions in relation to nutrient availability. In *Drosophila*, normal levels of autophagy play an important role in the homeostasis of certain terminally differentiated cells and stress survival (Juhasz et al., 2007; Neufeld and Baehrecke, 2008). Scott et al. (2004) demonstrated that starvation induces an autophagic response in *Drosophila* fat body, a nutrient storage and mobilization organ analogous to the vertebrate liver.

In this study we found that autophagy starts in precise coincidence with the onset of the non-feeding (wandering) period and mainly occurs during the early phase of the midgut remodeling process. Given that no water and food are taken by the animal after wandering stage, self-digestion of larval midgut cells and recycling of the breakdown products resulting from the autophagic process may provide a fundamental way to obtain materials and energy for regeneration and construction of pupal and adult structures. This hypothesis is supported by three pieces of evidence: i) we observed autophagic features in the degenerating yellow body, a mass of cells that does not disappear suddenly but is progressively degraded along the pupal phase. Consistently, the delayed and asynchronous death of yellow body cells that we have shown fits with a gradual supply of nutrients from the larval to the pupal

epithelium; ii) previous work demonstrated the presence of membrane transporters and hydrolytic enzymes in the newly formed pupal midgut of *Heliothis virescens*: the morpho-functional features of this epithelium are consistent with a recycling action of nutrients derived from the degradation of larval epithelium (Tettamanti et al., 2007b); iii) significant variations in protein concentration and ATP production take place in the time frame of the maximum occurrence of autophagy. Thus, the sudden decrease in protein content at wandering phase and the subsequent, massive increase in the amount of ATP suggest that autophagy determines the degradation of long-lived proteins in larval midgut to provide amino acids for ATP production by central carbon metabolism (Rabinowitz and White, 2010). These data are in agreement with a previous report showing that amino acid metabolism directly related to the tricarboxylic acid cycle is the primary source of energy in *B. mori* midgut (Parenti et al., 1985). Thus, these data indicate that, starting from wandering-spinning stage, autophagy intervenes to recycle nutrient materials derived from epithelial cells of the degenerating larval midgut to cope with lack of food during pupal phase.

In conclusion, our provide for the first time direct cellular, molecular and biochemical evidence of the involvement of autophagy in the midgut remodeling process during larval-adult transformation. Autophagy and apoptosis actively intervene in the degeneration process of the larval midgut epithelium and the two pathways might interact or cooperate to accomplish the irreversible process of the demise of this larval tissue. Most evidence indicates that in vertebrates autophagy mainly promotes cell survival, although it can play a role in the early phase of cell death (Jellinger and Stadelmann, 2001; Guillon-Munos et al., 2006; Eisenberg-Lerner et al., 2009; Shen and Codogno, 2011). Our data show that in silkworm midgut, autophagy has a pro-survival role to gain energy from larval cells that are no longer useful to the animal. The next challenge will be to assess whether autophagy also functions as a cell death mechanism in the midgut epithelium, thus demonstrating to be true autophagic cell death (Denton et al., 2009; Shen and Codogno, 2011).

REFERENCES

- Baehrecke E.H., 1996. *Ecdysone signaling cascade and regulation of Drosophila metamorphosis.* Arch. Insect Biochem. Physiol.; 33: 231-244.
- Baldwin K.M., Hakim R.S., 1991. *Growth and differentiation of the larval midgut epithelium during molting in the moth,* Manduca sexta. Tissue Cell; 23: 411-422.
- Baldwin K.M., Hakim R., Loeb M., Sadrud-Din S., 1996. *Midgut development.* In: Lehane M.J., Billingsley P.F. (Eds) *Biology of the insect midgut.* Chapman and Hall, London, pp 31-54.
- Barbehenn R.V., Kristensen N.P., 2003. *Digestive and escretory systems.* In: Kristensen N.P. (ed.) *Lepidoptera, moths and butterflies. Vol. 2: Morphology, Physiology, and Development.* Handbuch der Zoologie/Handbook of Zoology IV/36. Walter de Gruyter, Berlin and New York, pp 165-187.
- Barth J.M., Szabad J., Hafen E., Köhler K., 2011. *Autophagy in Drosophila ovaries is induced by starvation and is required for oogenesis.* Cell Death Differ.; 18: 915-924.
- Batistaou A., Greene L.A., 1993. *Internucleosomal DNA cleavage and neuronal cell survival/death.* J. Cell Biol.; 122: 523-532.
- Bernales S., Schuck S., Walter P., 2007. *Selective autophagy of the endoplasmic reticulum.* Autophagy; 3: 285-287.
- Berry D.L., Baehrecke E.H., 2007. *Growth arrest and autophagy are required for salivary gland cell degradation in* Drosophila. Cell.; 131: 1137-1148.
- Bradford M.M., 1976. *A rapid and sensitive method for the quantitation of microgram quantities of protein utilizing the principle of protein-dye binding.* Anal. Biochem.; 72: 248-254.
- Buzgariu W., Chera S., Galliot B., 2008. *Methods to investigate autophagy during starvation and regeneration in hydra.* Methods Enzymol.; 451: 409-437.
- Cakouros D., Daish T.J., Kumar S., 2004. *Ecdysone receptor directly binds the promoter of the Drosophila caspase dronc, regulating its expression in specific tissues*. J. Cell Biol.; 165: 631-640.
- Cappellozza L., Cappellozza S., Saviane A., Sbrenna G., 2005. *Artificial diet rearing system for the silkworm* Bombyx mori *(Lepidoptera: Bombycidae): effect of*

vitamin C deprivation on larval growth and cocoon production. Appl. Entomol. Zool.; 40: 405-412.

- Cardoso T.C., Castanheira T.L.L., Teixeira M.C.B., Rosa A.C.G., Hirata K.Y., Astolphi R.D., et al., 2008. *Validation of an immunohistochemistry assay to detect turkey coronavirus: a rapid and simple screening tool for limited resource settings.* Poultry Sci.; 87: 1347-1352.
- Casartelli M., Leonardi M.G., Fiandra L., Parenti P., Giordana B., 2001. *Multiple transport pathways for dibasic amino acids in the larval midgut of the silkworm* Bombyx mori. Insect Biochem. Mol. Biol.; 31: 621-632.
- Chang Y.Y., Neufeld T.P., 2010. *Autophagy takes flight in Drosophila.* FEBS Lett.; 584: 1342-1349.
- Chapman R.F., 1998. *The insects: structure and function.* 4. ed. Harvard University Press, Cambridge.
- Chiarelli R., Agnello M., Roccheri M.C., 2011. *Sea urchin embryos as a model system for studying autophagy induced by cadmium stress*. Autophagy; 7: 1028-1034.
- Clarke P.G., 1990. *Developmental cell death: morphological diversity and multiple mechanisms.* Anat. Embryol.; 181: 195-213.
- Conradt B., 2009. *Genetic control of programmed cell death during animal development*. Annu. Rev. Genet.; 43: 493-523.
- Codogno P.L, Meijer A.J., 2006. *Atg5: more than an autophagy factor*. Nat. Cell Biol.; 8: 1045-1047.
- Cooper D.M., Granville D.J., Lowenberger C., 2009. *The insect caspase*. Apoptosis; 14: 247-256.
- Cotter T.G., Lennon S.V., Glynn J.G., Martin S.J., 1990. *Cell death via apoptosis and its relationship to growth, development and differentiation of both tumour and normal cells.* Anticancer Res.; 10: 1153-1159.
- Courtiade J., Pauchet Y., Vogel H., Heckel D.G., 2011. *A comprehensive characterization of the caspase gene family in insects from the order Lepidoptera.* BMC Genomics; 12: 357.
- Crowson R.A., 1981. *The biology of the Coleoptera*. Academic, London.

- de Eguileor M., Grimaldi A., Tettamanti G., Valvassori R., Leonardi M.G., Giordana B., et al., 2001. *Larval anatomy and structure of absorbing epithelia in the aphid parasitoid* Aphidius ervi *Haliday (Hymenoptera, Braconidae).* Arthropod Struct. Dev.; 30: 27-37.
- Dai J.D., Gilbert L., 1997. *Programmed cell death of the prothoracic glands of* Manduca sexta *during pupal-adult metamorphosis.* Insect Biochem. Mol. Biol.; 27: 69-78.
- Daish T.J., Mills K., Kumar S., 2004. *Drosophila caspase DRONC is required for specific developmental cell death pathways and stress-induced apoptosis.* Dev. Cell; 7: 909-915.
- Dartsch D.C., Schaefer A., Boldt S., Kolch W., Marquardt H., 2002. *Comparison of anthracycline-induced death of human leukemia cells: programmed cell death versus necrosis.* Apoptosis; 7: 537-548.
- Denton D., Shravage B., Simin R., Mills K., Berry D.L., Baehrecke E.H., et al., 2009. *Autophagy, not apoptosis, is essential for midgut cell death in Drosophila*. Curr. Biol.; 19: 1741-1746.
- Denton D., Shravage B., Simin R., Baehrecke E.H., Kumar S., 2010. *Larval midgut destruction in Drosophila*: *not dependent on caspases but suppressed by the loss of autophagy.* Autophagy; 6: 163-165.
- Dow J.A.T., 1986. *Solid/plant feeders: "phytophagous insects*". In *Insect midgut function*. Advances in insect physiology; 19: 222-327.
- Dupere-Minier G., Hamelin C., Desharnais P., Bernier J., 2004. *Apoptotic volume decrease, pH acidification and chloride channel activation during apoptosis requires CD45 expression in HPB-ALL T cells.* Apoptosis; 9: 543-551.
- Edinger A.L., Thompson C.B., 2004. *Death by design: apoptosis, necrosis and autophagy.* Curr. Opin. Cell Biol.; 16: 663-669.
- Eisenberg-Lerner A., Biallk S., Simon H.U., Klimchi A., 2009. *Life and death parters: apoptosis, autophagy and the cross-talk bettween them*. Cell Death Differ.; 16: 966-975.
- Endo Y., Nishiitsutsuji-Uwo J., 1981. *Gut endocrine cells in insects: the ultrastructure of the gut endocrine cells of the lepidopterous species.* Biomed. Res.; 2: 270-280.

- Fahrbach S.E., Nambu J.R., Schwartz L.M., 2005. *Programmed cell death in insect neuromuscular system during metamorphosis.* In: Gilbert L.I., Iatrou K., Gill S.S. (eds). *Comprehensive molecular insect science*, Vol. 2. Elsevier, Oxford, pp 165-198.
- Ferguson R.E., Carroll H.P., Harris A., Maher E.R., Selby P.J., Banks R.E., 2005. *Housekeeping proteins: a preliminary study illustrating some limitations as useful references in protein expression studies.* Proteomics; 5: 566-571.
- Galluzzi L., Aaronson S.A., Abrams J., Alnemri E.S., Andrews D.W., Baehrecke E.H., et al., 2009. *Guidelines for the use and interpretation of assays for monitoring cell death in higher eukaryotes*. Cell Death Differ.; 16: 1093-1107.
- Galluzzi L., Vitale I., Abrams J.M., Alnemri E.S., Baehrecke E.H., Blagosklonny M.V., et al., 2012. *Molecular definitions of cell death subroutines: recommendations of the Nomenclature Committee on Cell Death 2012.* Cell Death Differ.; 19: 107-120.
- Giordana B., Leonardi M.G., Casartelli M., Consonni P., Parenti P., 1998. *K (+)-neutral amino acid symport of* Bombyx mori *larval midgut: a system operative in extreme conditions.* Am. J. Physiol.; 274: R1361-1371.
- Goncu E., Parlak O., 2011. *The influence of juvenile hormone analogue, fenoxycarb on the midgut remodeling in* Bombyx mori *(L., 1758) (Lepidoptera: Bombycidae*) *during larval-pupal metamorphosis*. Turk. J. of Entomol.; 35: 179-194.
- Griswold A.J., Chang K.T., Runko A.P., Knight M.A., Min K.T., 2008. *Sir2 mediates apoptosis through JNK-dependent pathways in Drosophila*. Proc. Natl. Acad. Sci. USA; 105: 8673-8678.
- Guillon-Munos A., van Bemmelen M.X.P., Clarke P.G.H., 2006. *Autophagy can be a killer even in apoptosis-competent cells.* Autophagy; 2: 140-142.
- Hakim R.S., Baldwin K., Smagghe G., 2010. *Regulation of midgut growth, development and metamorphosis*. Annu. Rev. Entomol.; 55: 593-608.
- Hou Y.C., Chittaranjan S., Barbosa S.G., McCall K., Gorski S.M., 2008. *Effector caspase Dcp-1 and IAP protein Bruce regulate starvation-induced autophagy durin* Drosophila melanogaster *oogenesis.* J. Cell Biol.; 182: 1127-1139.
- Hu C., Zhang X. A., Teng Y.B., Hu H.X., Li W.F., 2010. *Structure of autophagy-related protein Atg8 from the silkworm* Bombyx mori. Acta Crystallogr. F; 66: 787-790.

- Humbert W., 1979. *The midgut of* Tomocerus minor *Lubbock (Isecta, collembola): ultrastructure, cytochemistry, ageing and renewal during a moulting cycle.* Cell Tissue Res.; 196: 39-57.
- Iwanaga M., Kang W.K., Kobayashi M., Maeda S., 2000. *Baculovirus infection blocks the progression of fat body degradation during metamorphosis in* Bombyx mori. Arch. Virol.; 145: 1763-1771.
- Jellinger K.A., Stadelmann C., 2001. *Problems of cell death in neurodegeneration and Alzheimer's Disease.* J. Alzheimers Dis.; 3: 31-40.
- Johnson E.M.Jr, Deckwerth T.L., 1993. *Molecular mechanisms of developmental neuronal death.* Annu. Rev. Neurosci.; 16: 31-46.
- Jiang C., Baehrecke E.H., Thummel C.S., 1997. *Steroid regulated programmed cell death during* Drosophila *metamorphosis.* Development; 124: 4673-4683.
- Jiang H., Edgar B.A., 2009. *EGFR signaling regulates the proliferation of Drosophila adult midgut progenitors.* Dvelopment; 136: 483-493.
- Judy K.J., Gilbert L.I., 1970. *Histology of the alimentary canal during the metamorphosis of* Hyalophora cecropia *(L.)*. J. Morphol.; 131: 277-300.
- Juhász G., Erdi B., Sass M., Neufeld T.P., 2007. *Atg7-dependent autophagy promotes neuronal health, stress tolerance, and longevity but is dispensable for metamorphosis in* Drosophila. Genes Dev.; 21: 3061-3066.
- Kerr J.F., Wyllie A.H., Currie A.R., 1972. *Apoptosis: a basic biological phenomenon with wide-ranging implications in tissue kinetics.* Br. J. Cancer; 26: 239-257.
- Kiguchi K., Agui N., 1981. *Ecdysteroid levels and developmental events during larval moulting in the silkworm,* Bombyx mori. J. Insect Physiol. 27: 805-812.
- Klionsky D.J., 2007. *Autophagy: from phenomenology to molecular understanding in less than a decade.*. Nat. Rev. Mol. Cell Biol.; 8: 931-937.
- Klionsky D.J., Abeliovich H., Agostinis P., Agrawal D.K., Aliev G., Askew D.S., et al., 2008. *Guidelines for the use and interpretation of assays for monitoring autophagy in higher eukaryotes*. Autophagy; 4: 151-175.
- Kőműves L., Sass M., Kovács J., 1985. *Autophagocytosis in the larval midgut cells of* Pieris brassicae *during metamorphosis*. Cell Tissue Res.; 240: 215-221.

- Kroemer G., Levine B., 2008. *Autophagic cell death: the story of a misnomer*. Nat. Rev. Mol. Cell Biol.; 9: 1004-1010.
- Kroemer G., Galluzzi L., Vandenabeele P., Abrams J., Alnemri E.S., Baehrecke E.H., et al., 2009. *Classification of cell death: recommendations of the Nomenclature Committee on Cell Death*. Cell Death Differ.; 16: 3-11.
- Lamkanfi M., Declercq W., Kalai M., Saelens X., Vandenabeele P., 2002. *Alice in caspase land. A phylogenetic analysis of caspases from worm to man.* Cell Death Differ.; 9: 358-361.
- Larsen W.J., 1976. *Cell remodelling in the fat body of an insect.* Tissue Cell.; 8: 73-92.
- Lee C.Y., Baehrecke E.H., 2001. *Steroid regulation of autophagic programmed cell death during development.* Development; 128: 1443-1455.
- Lee C.Y., Cooksey B.A.K., Baehrecke E.K., 2002. *Steroid regulation of midgut cell death during Drodophila development.* Dev. Biol.; 250: 101-111.
- Leonardi M.G., Casartelli M., Parenti P., Giordana B., 1998. *Evidence for a low-affinity, high-capacity uniport for amino acids in* Bombyx mori *larval midgut.* Am. J. Physiol.; 274: R1372-R1375.
- Levy S.M., Falleiros A.M.F., Gregório E.A., Arrebola N.R., Toledo L.A., 2004. *The larval midgut of* Anticarsia gemmatalis *(Hübner) (Lepidoptera: Noctuidae): light and electron microscopy studies of the epithelial cells.* Braz. J. Biol.; 64: 633-638.
- Li Q.R., Deng X.J., Yang W.Y., Huang Z.J., Tettamanti G., Cao Y, et al., 2010. *Autophagy, apoptosis, and ecdysis-related gene expression in the silk gland of the silkworm (*Bombyx mori*) during metamorphosis.* Can. J. Zool.; 88: 1169-1178.
- Livak K.J., Schmittgen T. D., 2001. *Analysis of relative gene expression data using real-time quantitative PCR and the 2(T)(-Delta Delta C) method.* Methods 25: 402-408.
- Lockshin R.A., Zakeri Z., 2004. *Apoptosis, autophagy, and more.* Int. J. Biochem. Cell. Biol.; 36: 2405-2419.
- Malagoli D., Abdalla F.C., Cao Y., Feng Q., Fujisaki K., Gregorc A., et al., 2010. *Autophagy and its physiological relevance in arthropods: Current knowledge and perspectives.* Autophagy; 6: 575-588.

- Manjithaya R., Nazarko T.Y., Farrè J.C., Subramani S., 2010. *Molecular mechanism and physiological role of pexophagy*. FEBS Lett.; 584: 1367-1373.
- Martinet W., De Meyer G.R., 2008. *Autophagy in atherosclerosis.* Curr. Atheroscler. Rep.; 10: 216-223.
- Martins G.F., Neves C.A., Campos L.A., Serrao J.E., 2006. *The regenerative cells during the metamorphosis in the midgut of bees.* Micron.; 37: 161-168.
- Meléndez A., Neufeld T.P., 2008. *The cell biology of autophagy in metazoans: a developing story*. Development; 135: 2347-2360.
- Micchelli C.A., Perrimon N., 2006. *Evidence that stem cells reside in the adult Drosophila midgut epithelium.* Nature; 439: 475-479.
- Mizushima N., Levine B., Cuervo A.M., Klionsky D.J., 2008. *Autophagy fights disease through cellular self-digestion.* Nature; 451: 1069-1075.
- Mizushima N., Yoshimori T., Levine B., 2010. *Methods in mammalian autophagy research.* Cell; 140: 313-326.
- Moss W.D., 1983. *Acid phosphatases*. In: Bergmeyer J., Grassi M. (Eds). *Esterases, glycosidases, lyases, ligases.* Vol. 4: *Methods of enzymatic analysis*. Verlag-Chemie, Weinheim: 92-106.
- Mpakou V.E., Nezis I.P., Stravopodis D.J., Margaritis L.H., Papassideri I.S., 2006. *Programmed cell death of the ovarian nurse cells during oogenesis of the silkmoth* Bombyx mori*.* Dev. Growth Differ.; 48: 419-428.
- Narendra D., Tanaka A., Suen D.F., Youle R.J., 2008. *Parkin is recruited selectively to impaired mitochondria and promotes their autophagy.* J. Cell Biol.; 183: 795-803.
- Neufeld T.P., Baehrecke E.H., 2008. *Eating on the fly: function and regulation of autophagy during cell growth, survival and death in Drosophila*. Autophagy; 4: 557-562.
- Nezis I.P., Shravage B.V., Sagona A.P., Lamark T., Bjørkøy G., Johansen T., et al., 2010. *Autophagic degradation of dBruce controls DNA fragmentation in nurse cells during late* Drosophila melanogaster *oogenesis.* J. Cell Biol.; 190: 523-531.
- Nishiura J.T., Smouse D., 2000. *Nuclear and cytoplasmic changes in the* Culex pipens *(Diptera: Culicidae) alimentary canal during metamorphosis and their relationship to programmed cell death.* Ann. Entomol. Soc. Am.; 93: 282-290.

- Ohlstein B., Spradling A., 2006. *The adult Drosophila posterior midgut is maintained by pluripotent stem cells.* Nature; 439: 470-474.
- Parenti P., Giordana B., Sacchi V.F., Hanozet G.M., Guerritore A., 1985. *Metabolic activity related to the potassium pump in the midgut of* Bombyx mori *larvae.* J. Exp. Biol.; 116: 69-78.
- Parthasarathy R., Palli S.R., 2007a. *Stage- and cell-specific expression of ecdysone receptors and ecdysone-induced transcription factors during midgut remodeling in the yellow fever mosquito*, Aedes aegypti. Insect Physiol.; 53: 216-229.
- Parthasarathy R., Palli S.R., 2007b. *Developmental and hormonal regulation of midgut remodeling in a lepidopteran insect,* Heliothis virescens*.* Mech. Dev.; 124: 23-34.
- Park M.S., Takeda M., 2008. *Starvation suppresses cell proliferation that rebounds after refeeding in the midgut of the American cockroach,* Periplaneta americana*.* J. Insect Physiol.; 54: 386-392.
- Park Y.E., Hayashi Y.K., Bonne G., Arimura T., Noguchi S., Nonakal I., et al., 2009. *Autophagic degradation of nuclear components in mammalian cells.* Autophagy; 5: 795-804.
- Pearse E.A.G., 1960. *Histochemistry, theoretical and applied.* Little, Brown and Company, Boston.
- Rabinowitz J.D., White E., 2010. *Autophagy and metabolism.* Science; 330: 1344-1348.
- Reddy R.M., Prasad G.V., 2011. *Silk-the prospective and compatible bio-material for advanced functional applications*. Trends Appl. Sci. Res.; 6: 89-95.
- Riddiford L.M., Palli S.R., Hiruma K., 1990. *Hormonal control of sequential gene expression in* Manduca *epidermis.* Prog. Clin. Biol. Res.; 342: 226-231.
- Riddiford L.M., 1993. *Hormone receptors and the regulation of insect metamorphosis.* Receptor; 3: 203-209.
- Romero-Calvo I., Ocon B., Martinez-Moya P., Suarez M.D., Zarzuelo A., Martinez-Augustin O., et al., 2010. *Reversible Ponceau staining as a loading control alternative to actin in Western blots.* Anal. Biochem.; 401: 318-320.

- Rybczynski R., 2005. *Prothoracic hormone.* In: Gilbert L.I., Iatrou K., Gill S.S. (Eds) Endocrinology. Vol. 3: *comprehensive molecular insect science*. Elsevier Pergamon, Oxford; pp 61-123.
- Russel V.W., Dunn P.E., 1991. *Lysozyme in the midgut of* Manduca sexta *during metamorphosis.* Arch. Insect Biochem. Physiol.; 17: 67-80.
- Sadasivan S., Waghray A., Larner S.F., Dunn W.A.Jr, Hayes R.L., Wang K.K., 2006. *Amino acid starvation induced autophagic cell death in PC-12 cells: evidence for activation of caspase-3 but not calpain-1.* Apoptosis; 11: 1573-1582.
- Sadrud-Din S., Hakim R., Loeb M., 1994. *IProloferation and differentiation of midgut epithelial cells from* Manduca sexta *in vitro.* Invertebr. Reprod. Dev.; 26: 197-204.
- Sadrud-Din S., Loeb M., Hakim R., 1996. *In vitro differentiation of isolated stem cells from the midgut of* Manduca sexta *larvae.* J. Exp. Biol.; 199: 319-325.
- Sambrook J., Fritsch E.F., Maniatis T., 1989. *Detection and analysis of proteins expressed from cloned genes.* In: *Molecular cloning - A laboratory manual*. Cold Spring Harbor Laboratory Press, New York: 18.11-18.88.
- Santos C.D., Ribeiro A.F., Ferreira C., Terra W.R., 1984. *The larval midgut of the cassava hornworm (*Erinnyis ello*).* Cell Tissue Res.; 237: 565-574.
- Schweichel J.U., Merker H.J., 1973. *The morphology of various types of cell death in prenatal tissues.* Teratology; 7: 253-266.
- Scott R.C., Schuldiner O., Neufeld T.P., 2004. *Role and regulation of starvation-induced autophagy in the Drosophila fat body.* Dev. Cell; 7: 167-178.
- Scott R.C., Juhasz G., Neufeld T.P., 2007*. Direct induction of autophagy by Atg1 inhibits cell growth and induces apoptotic cell death.* Curr. Biol.; 17: 1-11.
- Shelly S., Lukinova N., Bambina S., Berman A., Cherry S., 2009. *Autophagy is an essential component of Drosophila immunity against vesicular stomatitis virus.* Immunity; 30: 588-598.
- Shen H.M., Codogno P., 2011. *Autophagic cell death: Loch Ness monster or endangered species?* Autophagy; 7: 457-465.
- Spies A.G., Spence K.D., 1985. *Effect of a sublethal* Bacillus thuringiensis *crystal endotoxin treatment on the larval midgut of a moth,* Manduca sexta*: a SEM study.* Tissue Cell; 17: 379-394.

- Strange R., Li F., Saurer S., Burkhardt A., Friis R.R., 1992. *Apoptotic cell death and tissue remodelling during mouse mammary gland involution.* Development; 115: 49-58.
- Sumithra P., Britto C.P., Krishnan M., 2010. *Modes of cell death in the pupal perivisceral fat body tissue of the silkworm* Bombyx mori *L.* Cell Tissue Res.; 339: 349-358.
- Tanaka H., Ishibashi J., Fujita K., Nakajima Y., Sagisaka A., Tomimoto K., et al., 2008. *A genome-wide analysis of genes and gene families involved in innate immunity of* Bombyx mori. Insect Biochem. Mol. Biol.; 38: 1087-1110.
- Terashima J., Yasuhara N., Iwami M., Sakurai S., 2000. *Progremmed cell death triggered by insect steroid hormone, 20-hydroxyecdysone, in the anterior silk gland of the silkworm,* Bombyx mori. Dev. Genes Evol.; 11: 545-558.
- Tettamanti G., Grimaldi A., Casartelli M., Ambrosetti E., Ponti B., Congiu T., et al., 2007a. *Programmed cell death and stem cell differentiation are responsible for midgut replacement in* Heliothis virescens *during prepupal instar*. Cell Tissue Res.; 330: 345-359.
- Tettamanti G., Grimaldi A., Pennacchio F., de Eguileor M., 2007b. *Lepidopteran larval midgut during prepupal instar: digestion or self-digestion?* Autophagy; 3: 630-631.
- Tettamanti G., Malagoli D., 2008. *In vitro methods to monitor autophagy in Lepidoptera*. Method. Enzymol.; 451: 685-709.
- Tettamanti G., Cao Y., Feng Q., Grimaldi A., de Eguileor M., 2011. *Autophagy in Lepidoptera: more than old wine in new bottle*. Invert. Surv. J.; 8: 5-14.
- Terra W.R., 2001. *The origin and functions of the insect peritrophic membrane and peritrophic gel.* Arch. Insect Biochem. Physiol.; 47: 47-61.
- Terra W.R., Ferreira C., 2005. *Biochemistry of digestion*. In: Gilbert L.I., Iatrou K., Gill S.S. (eds). *Comprehensive molecular insect science.* Elsevier Pergamon, Oxford, pp 171-224.
- Thummel C.S., 2001. *Steroid-triggered death by autophagy.* Bioessays; 23: 677-682.
- Ulukaya E., Acilan C., Yilmaz Y., 2011. *Apoptosis: why and how does it occur in biology?* Cell Biochem. Funct.; 29: 468-480.

- Uwo F.M., Ui-Tei K., Park P., Takeda M., 2002. *Replacement of midgut epithelium in greater wax moth,* Galleria mollonela*, during larval-pupal moult*. Cell Tissue Res.; 308: 319-331.
- Vilaplana L., Pascual N., Perera N., Belle X., 2007. *Molecular characterization of an inhibitor of apoptosis in the Egyptian armyworm,* Spodoptera littoralis*, and midgut cell death during the metamorphosis*. Insect Biochem. Mol. Biol.; 37: 1241-1248.
- Wigglesworth V.B., 1972. *Digestion and nutrition*. In: *The principles of insect physiology.* Chapman & Hall, London, pp 476-552.
- Waku Y., Sumimoto K.I., 1971. *Metamorphosis of midgut epithelial cells in the silkworm (*Bombyx mori *L.) with special regard to the calcium salt deposits in the cytoplasm. I. Light Mycroscopy.* Tissue Cell; 3: 127-136.
- Wang J., Xia Q., He X., Dai M., Ruan J., Chen J., et al., 2005. *SilkDB: a knowledgebase for silkworm biology and genomics.* Nucleic Acids Res.; 33(Database issue): D399-402.
- Welinder C., Ekblad L., 2011. *Coomassie staining as loading control in Western blot analysis.* J. Proteome Res.; 10: 1416-1419.
- Wieczorek H., Grber G., Harvey W.R., Huss M., Merzendorfer H., Zeiske W., 2000. *Structure and regulation of insect plasma membrane H(+)V-ATPase.* J. Exp. Biol.; 203: 127-135.
- Wu Y., Parthasarathy R., Bai H., Palli S.R., 2006. *Mechanisms of midgut remodeling: juvenile hormone analog methoprene blocks midgut metamorphosis by modulating ecdysone action.* Mech Dev; 123: 530-547.
- Yin V.P., Thummel C.S., 2005. *Mechanisms of steroid-triggered programmed cell death in* Drosophila. Semin. Cell Dev. Biol.; 16: 237-243.
- Yla-Anttila P., Vihinen H., Jokitalo E., Eskelinen E.L., 2009. *Monitoring autophagy by electron microscopy in mammalian cells.* Methods Enzymol.; 452: 143-164.
- Yousefi S., Perozzo R., Schmid I., Ziemiecki A., Schaffner T., Scapozza L., et al. 2006. *Calpain-mediated cleavage of Atg5 switches autophagy to apoptosis.* Nat. Cell Biol.; 8: 1124-1132.
- Yue Z.Y., Jin S.K., Yang C.W., Levine A.J., Heintz N., 2003. *Beclin 1, an autophagy gene essential for early embryonic development, is a haploinsufficient tumor suppressor*. Proc. Natl. Acad. Sci. USA; 100: 15077-15082.

- Zanuncio J.C., Nascimento E.C., Garcia J.F., Zanuncio T.V., 1994. *Major lepidopterous of eucalypt in southeast Brazil.* For. Ecol. Manag.; 45: 53-63.
- Zanuncio J.C., Saavedra J.L.D., Oliveira H.N., Degheele D., Clercq P.D., 1996. *Development of the predatory stinkbug* Brontocoris tabidus *(Signoret) (Heteroptera: Pentatomidae) on different proportions of an artificial diet and pupae of* Tenebrio molitor *L. (Coleoptera: Tenebrionidae).* Bioc. Sci. Technol.; 6: 619-625.
- Zanuncio J.C., Saavedra J.L.D., Zanuncio T.V., Santos G.P., 1996-1997. *Incremento en el peso de ninfas y adultos de* Podisus nigrispinus *(Heteroptera: Pentatomidae) alimentados con dos tipos de larvas.* Rev. Biol. Trop.; 45: 241-245.
- Zhang X., Hu Z.Y., Li W.F., Li Q.R., Deng X.J., Yang W.Y., et al., 2009. *Systematic cloning and analysis of autophagy-related genes from the silkworm* Bombyx mori. BMC Mol. Biol.; 10: 50.
- Zhang J.Y., Pan M.H., Sun Z.Y., Huang S.J., Yu Z.S., Liu D., et al., 2010. *The genomic underpinnings of apoptosis in the silkworm*, Bombyx mori. BMC Genomics; 11: 611.
- Zhou S., Zhou Q., Liu Y., Wang S., Wen D., He Q., et al., 2010. *Two Tor genes in the silkworm* Bombyx mori. Insect Mol. Biol.; 19: 727-735.

FIGURES

Fig. 1 Morphological and structural changes of the alimentary canal of *B. mori* during metamorphosis

The aspect of silkworm larval midgut deeply changes during larval-adult transformation. **A-D** During fifth larval instar (**A, B**) and at wandering stage (**C, D**), the gut is a long and thin tube. **E, F** Starting from spinning stage, the alimentary canal is modified and the midgut region (*arrow*) becomes shorter and with folds on the outer surface. **G-J** These modifications are more dramatic during pupal stage. **K, L** In the adult the midgut is a small conical structure. s: rectal sac. Bars: **B, D, F,H, J** 0,5 cm; **L** 250 nm.

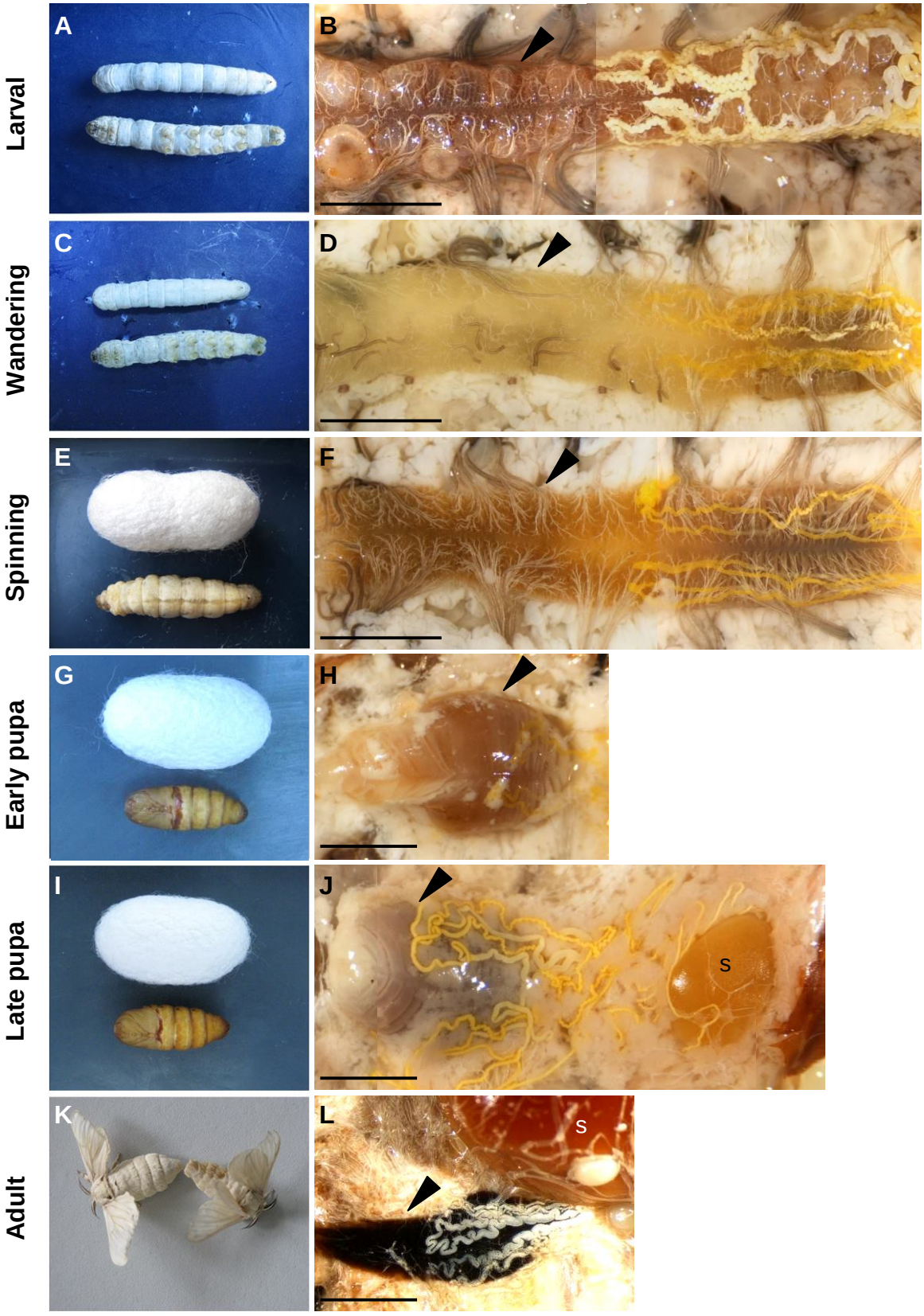
Larval
Wandering
Spinning
Early pupa
Late pupa
Adult
A
B
C
D
E
F
G
H
I
J
K
L
S
S

Fig. 2 Structure of larval epithelium and stem cell activation
A, B During fifth larval instar *B. mori* midgut consists of a monolayered epithelium in which columnar (*c*) and goblet (*g*) cells are readily identifiable. Columnar cells show a thick luminal brush border (*b*), whereas goblet cells are characterized by a goblet cavity (*arrows*) covered by closely arranged microvilli (*mv*). Sparse stem cells (*arrowheads*) are scarcely represented and localized in the basal region of the midgut epithelium. The midgut monolayer is surrounded by a thin layer of muscle fibers and tracheae (*m*). **C, D** SEM analysis evidences that nuclei of larval epithelial cells show uncondensed chromatin (*n,* **C**). Mitochondria (*arrows*) and rough endoplasmic reticulum (*arrowheads*) are detectable in the cytoplasm (**D**). **E, F** Some areas are characterized by apical blebs, cell swelling, and ruptures on the luminal side of the midgut. **G, H** Immunohistochemical analysis performed with anti-Phospho-Histone H3 antibody demonstrates that active proliferation of stem cells (*arrowheads*) initiates at wandering stage. *l* lumen, *e* larval midgut epithelium. Bars: **A, G** 25 µm; **B, E** 10 µm; **C, F** 2 µm; **D** 500 nm; **H** 100 µm.

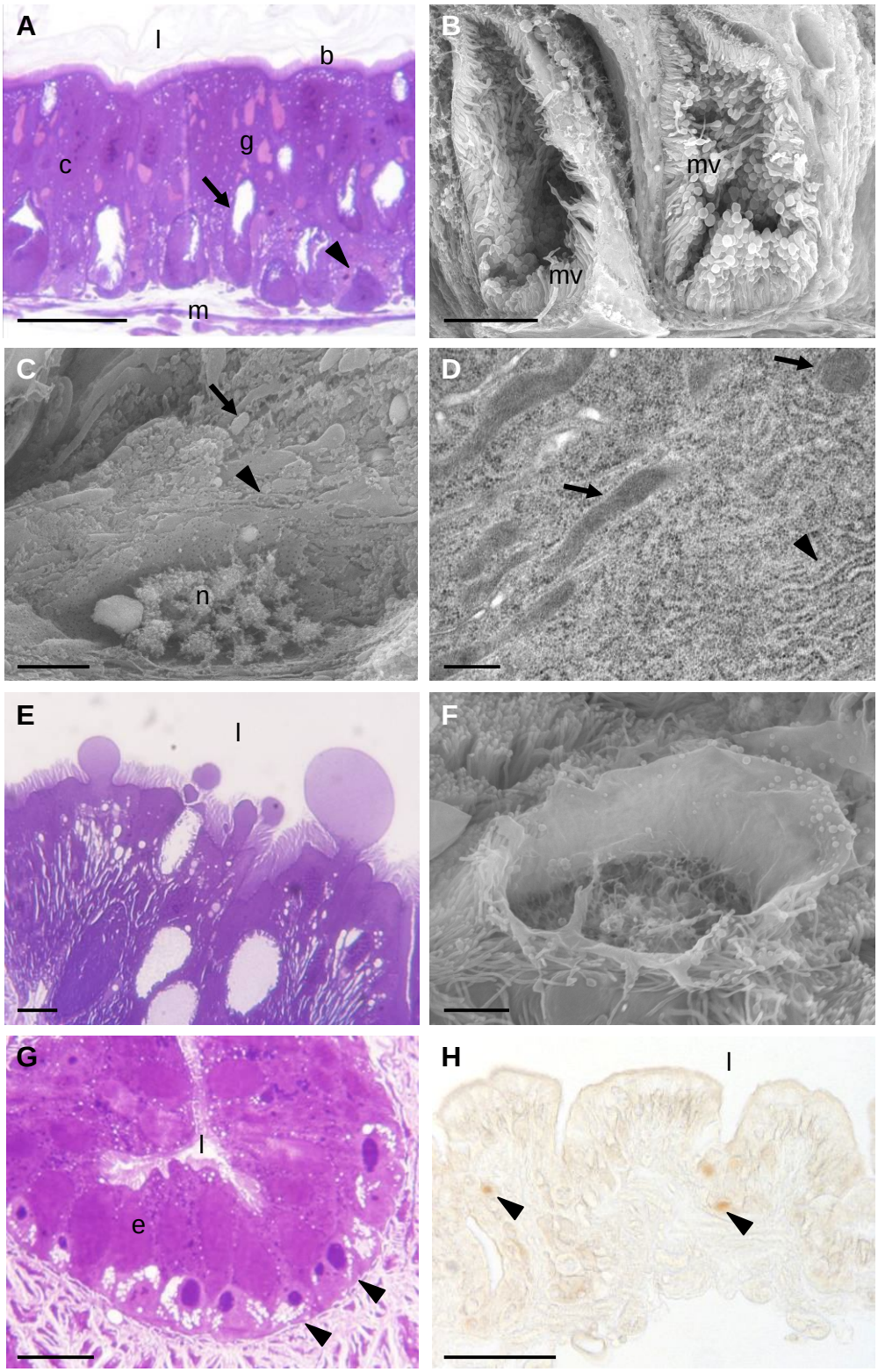
A
l
b
g
c
m
B
mv
mv
C
n
D
E
l
F
G
l
e
H
l

Fig. 3 Spinning phase and stem cell differentiation
A-D Stem cells proliferate and differentiate forming a continuous layer on the basal side of the midgut, thus pushing the old epithelium (*yb*) toward the lumen; the midgut wall undergoes a gradual thickening. **A, B** At SD1 phase larval midgut epithelium cells (*e*) are characterized by initial degeneration but still keeps in close contact with the new cell layer (*bracket*). **C, D** At SD2 phase the old epithelium (*yb*) detaches from the new pupal epithelium, and still exhibits microvilli (*mv*). **A, D, E, F** Stem cells show a cytoplasmic compartment (*c*) lined by short projections (*arrows*) which become shorter and thinner at SD2 phase (*arrowheads*). l: lumen. Bars: **A** 25 µm; **B, D, F** 10 µm; **C** 100 µm; **E** 5 µm.

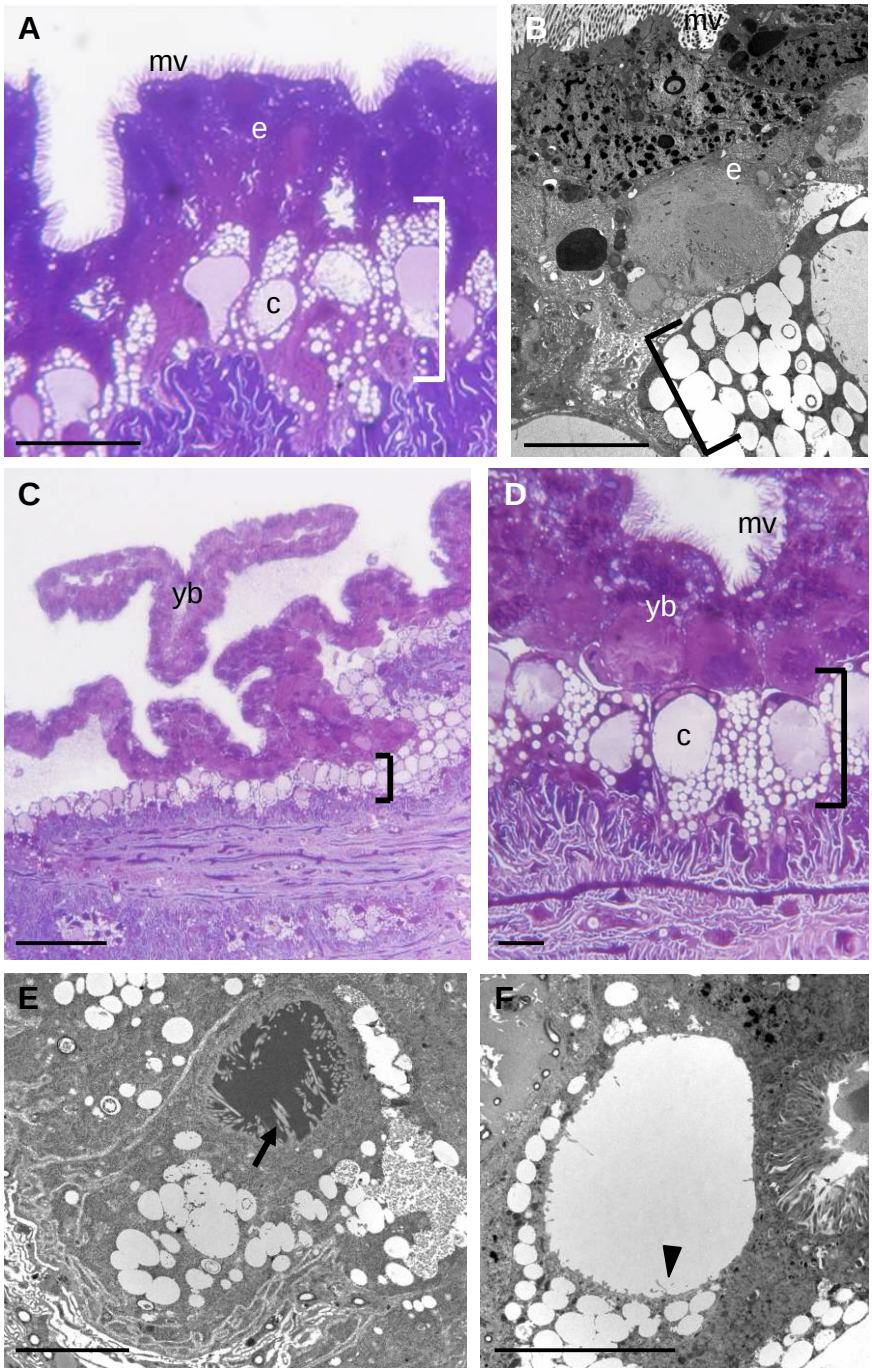
A
mv
e
c
B
mv
e
C
yb
D
mv
yb
c
E
F

Fig. 4 Formation of prepupal midgut and organization of pupal midgut

A A new compact layer formed by stem cells, the prepupal midgut, is visible (*bracket*). **B-D** The new epithelium is remodelled during larval-adult transformation leading to the formation of a well-organized pupal midgut (*bracket*), which shows a brush border (*b*) and a junctional system (*white arrowheads*). Yellow body (*yb*) is visible inside the lumen. **C-J** Within these cells there are round cytoplasmic structures of various size (*white arrows*) containing lipid droplets (*f*) surrounded by glycogen granules (*g*), several vesicles, a great amount of mithocondria (*black arrowheads*), and concentrically laminated spherites (*black arrows*). **C, H** Throughout the cell layer vesicles of various size are visible among microvilli during exocytosis (*white arrows*). *l* lumen. Bars:**A** 25 µm; **B** 100 µm; **C, G** 10 µm; **D** 1 µm; **E, H, I, J** 2 µm; **F** 5 µm.

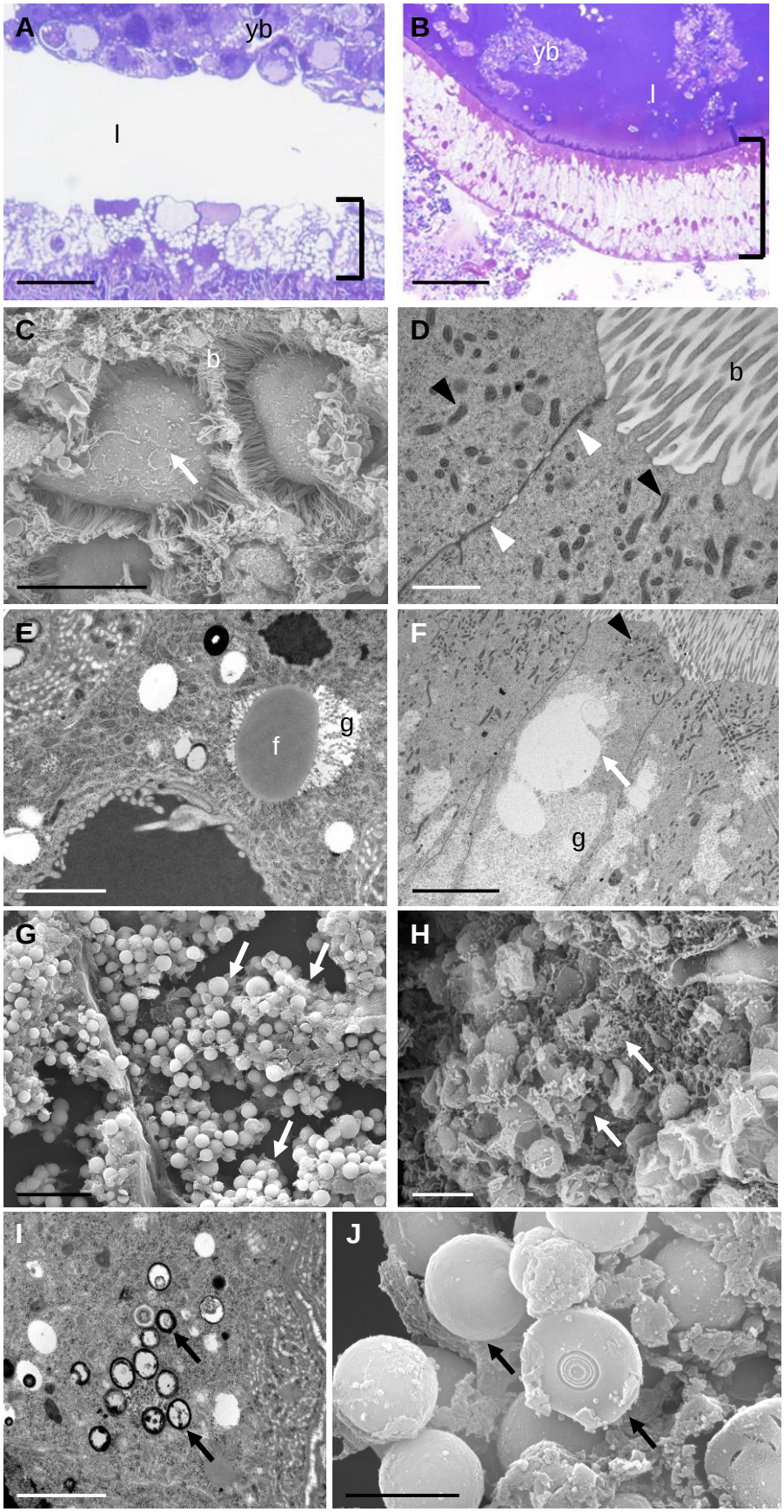
A
yb
l
B
yb
l
C
b
D
b
E
f
g
F
g
G
H
I
J

Fig. 5 Degeneration of larval midgut epithelium
A Yellow body (*yb*) is recognizable inside the lumen of the new pupal midgut as a compact mass of cells which progressively degrades until desappearance. **B, C** At early stages of degeneration contacts among epithelial cells are still maintained (*white arrowheads*), but progressively their organization change: old columnar and goblet cells shrink and undergo ruptures (*arrows*). **D, E** TEM and SEM images demonstrate the presence of condensed chromatin in nuclei within yellow body cells (*black arrowheads*). *l* lumen. Bars: **A, B** 10 µm; **C, D** 5 µm; **E** 2 µm.

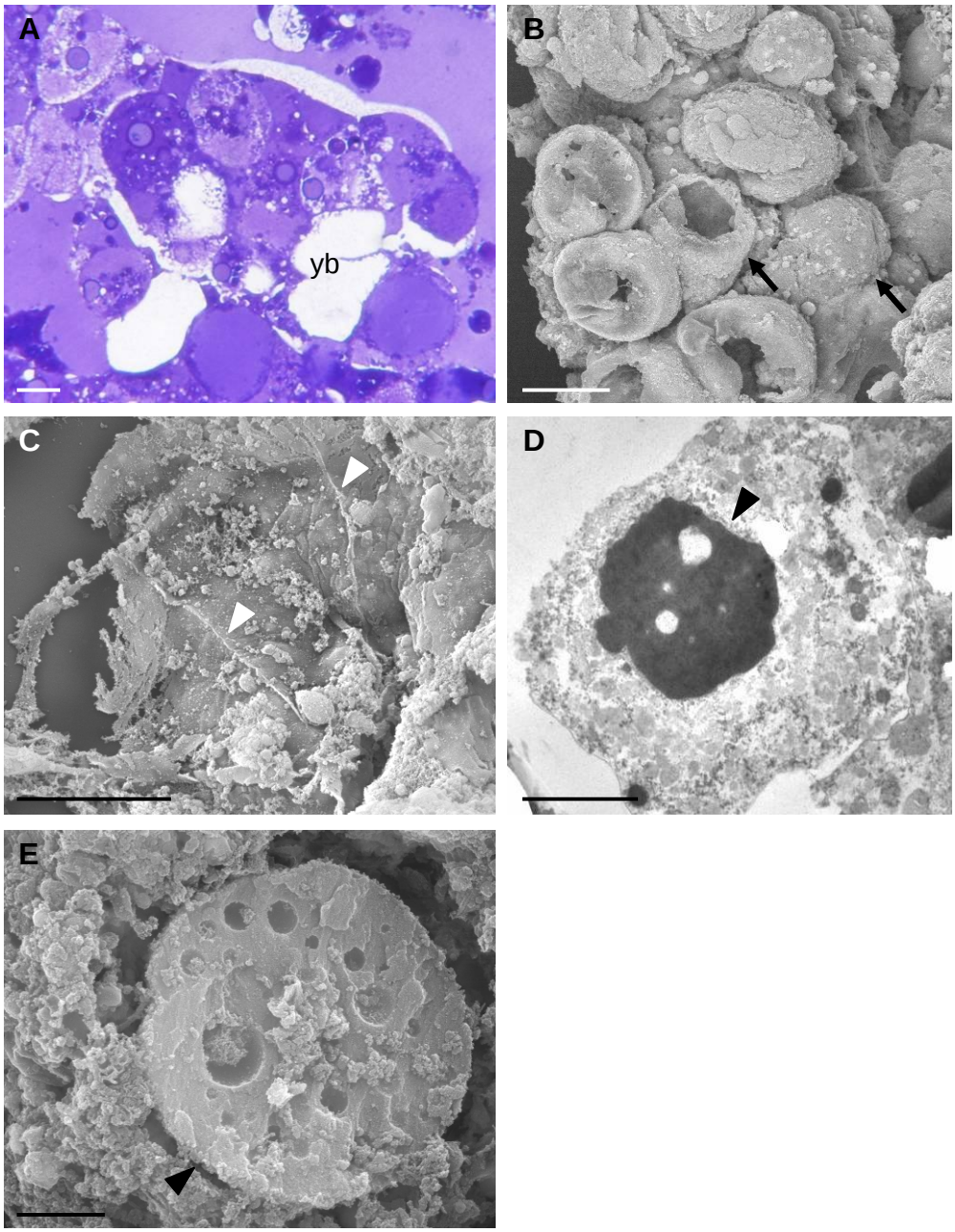
A
yb
B
C
D
E

Fig. 6 Organization of adult midgut
A, B The midgut epithelium of the adult is narrow and characterized by a brush border composed of rare and flattened microvilli (mv). Abundant endoplasmic reticulum (*white arrowheads*) and mitochondria (*white arrows*) are present. **C, D** Small isolated cells are localized in the basal region of the epithelium (*black arrowheads*). **E, F** A continuous exocytosis of several vesicles is visible. Boxed areas in (**C**) and (**E**) are shown at higher magnification in (**D**) and (**F**), respectively. *l* lumen. Bars: **A** 50 µm; **B, F** 2 µm; **C** 20 µm; **D, E** 10 µm.

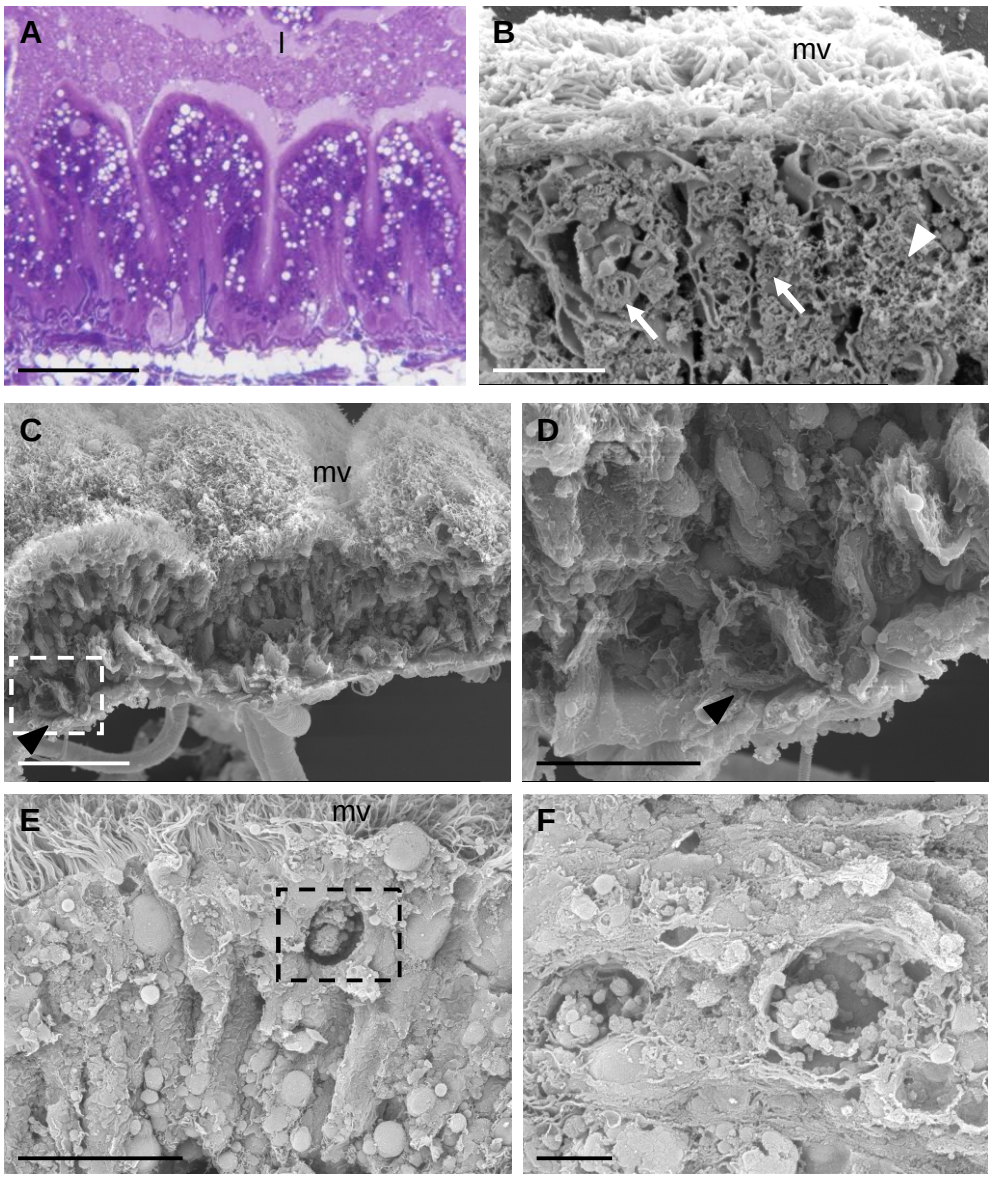
A
l
B
mv
C
mv
D
E
mv
F

Fig. 7 Histochemical characterization of larval and prepupal midguts: PAS (glycogen detection)
PAS reaction reveals that, although glycogen granules (*arrows)* are visible within larval midgut epithelium (**A, B**), at advanced stages of development (**C-G**) only the cells of the pupal epithelium (*brackets*) are positive to the staining and no reactivity is detectable in the yellow body (*yb*). *l* lumen, *e* larval midgut epithelium. Bars: **A, E** 100 µm; **B, C, D, F, G** 10 µm.

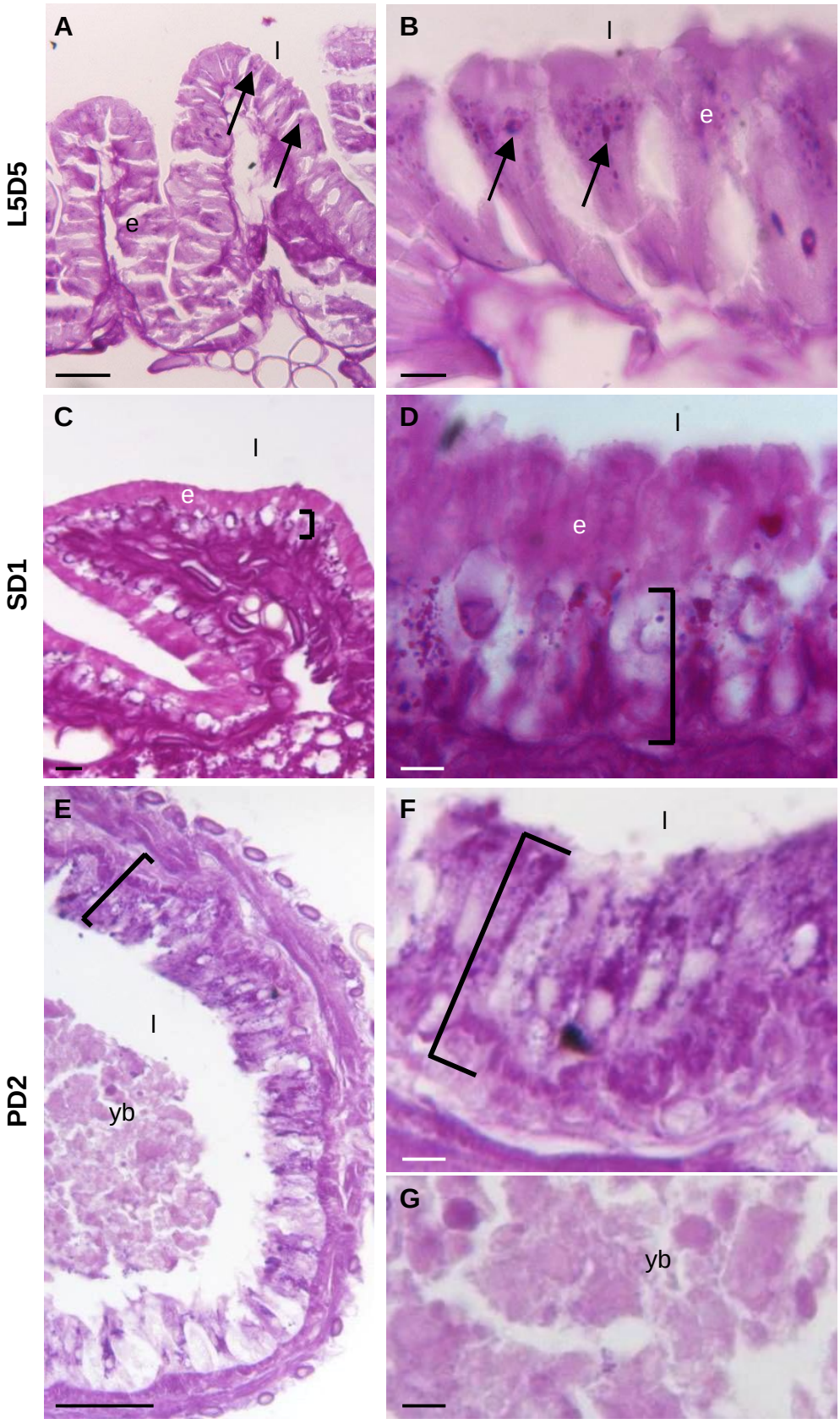
L5D5
SD1
PD2
A
B
C
D
E
F
G
l
e
yb

Fig. 8 Histochemical characterization of larval and prepupal midguts: NADH-TR (marker for mithocondrial activity)
A, B Staining for NADH-TR is strong in larval midgut epithelium (*arrows*). **C-H** After the generation of the new pupal midgut (*bracket*) a progressive reduction of metabolic activity is evident in larval midgut cells until their complete degeneration within the yellow body (*yb*). **C-J** At spinning stage (**C-E**) high mitochondrial activity is visible in the new midgut epithelium and the positivity to the reaction continue to be detectable in the cells of the pupal and adult midgut epithelium (**F-J**, *bracket*). *l* lumen, *e* larval midgut epithelium. Bars: **A, C, F, I** 100 µm; **B, D, E, G, H, J** 10 µm.

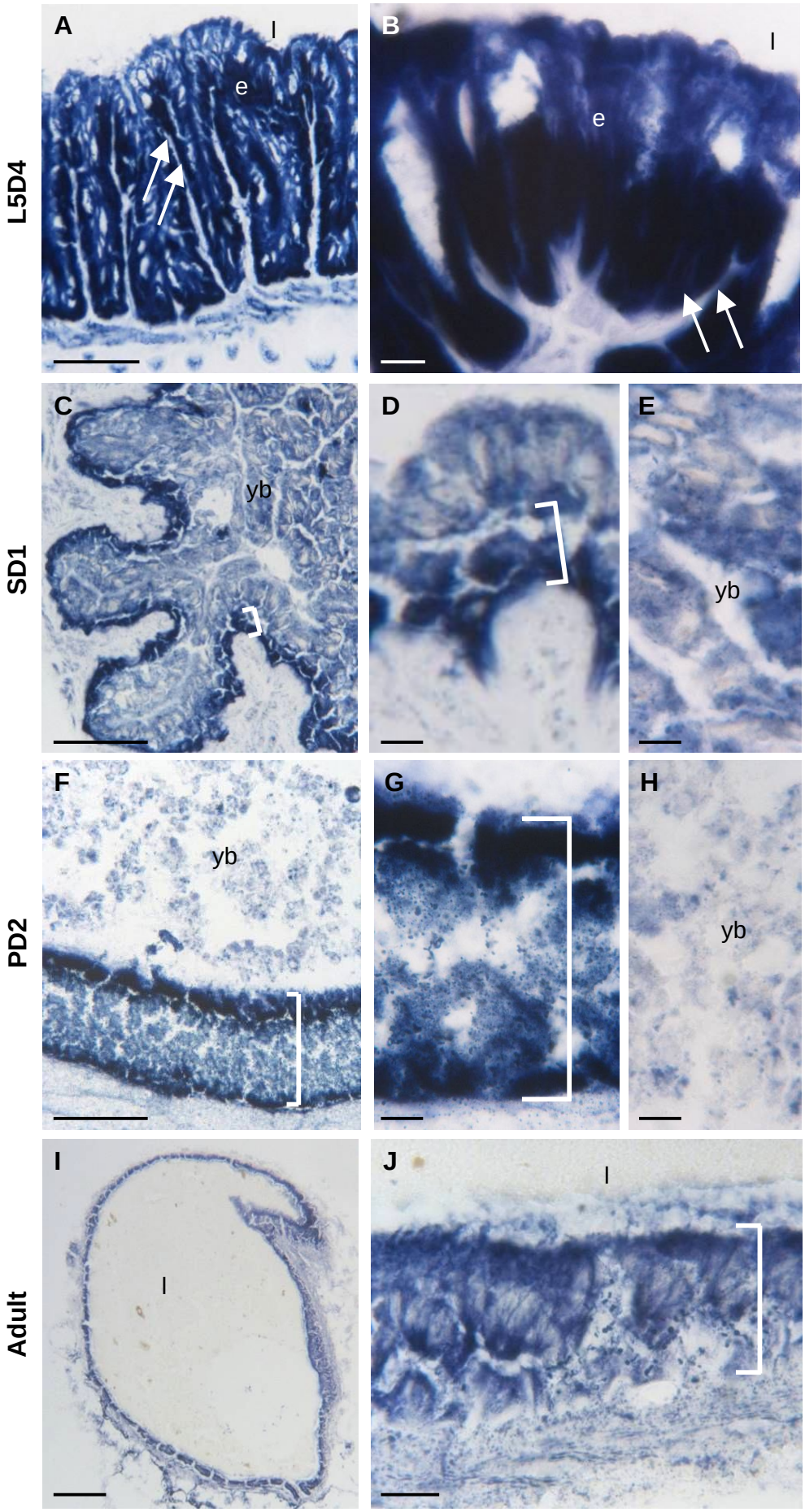
L5D4
SD1
PD2
Adult
A
B
C
D
E
F
G
H
I
J
l
e
yb

Fig. 9 Morphological study of the autophagic process

TEM analysis of representative autophagic features that can be observed in larval midgut cells from spinning stage to pupal phase. **A, C** Autophagosomes (*a*) are characterized by a double-limiting membrane (*arrowheads*). **B, D** Autolysosomes (*a*) contain degraded organelles and are surrounded by lysosomes (*arrows*). **E** Myelin-like structures (*arrowheads*) that contain whorls of membranes can also be observed in these cells. Boxed area in (**A**) and (**B**) are shown at higher magnification in (**C**) and (**D**), respectively. Bars: **A, D** 500 nm; **B, E** 2 µm ; **C** 200 nm.

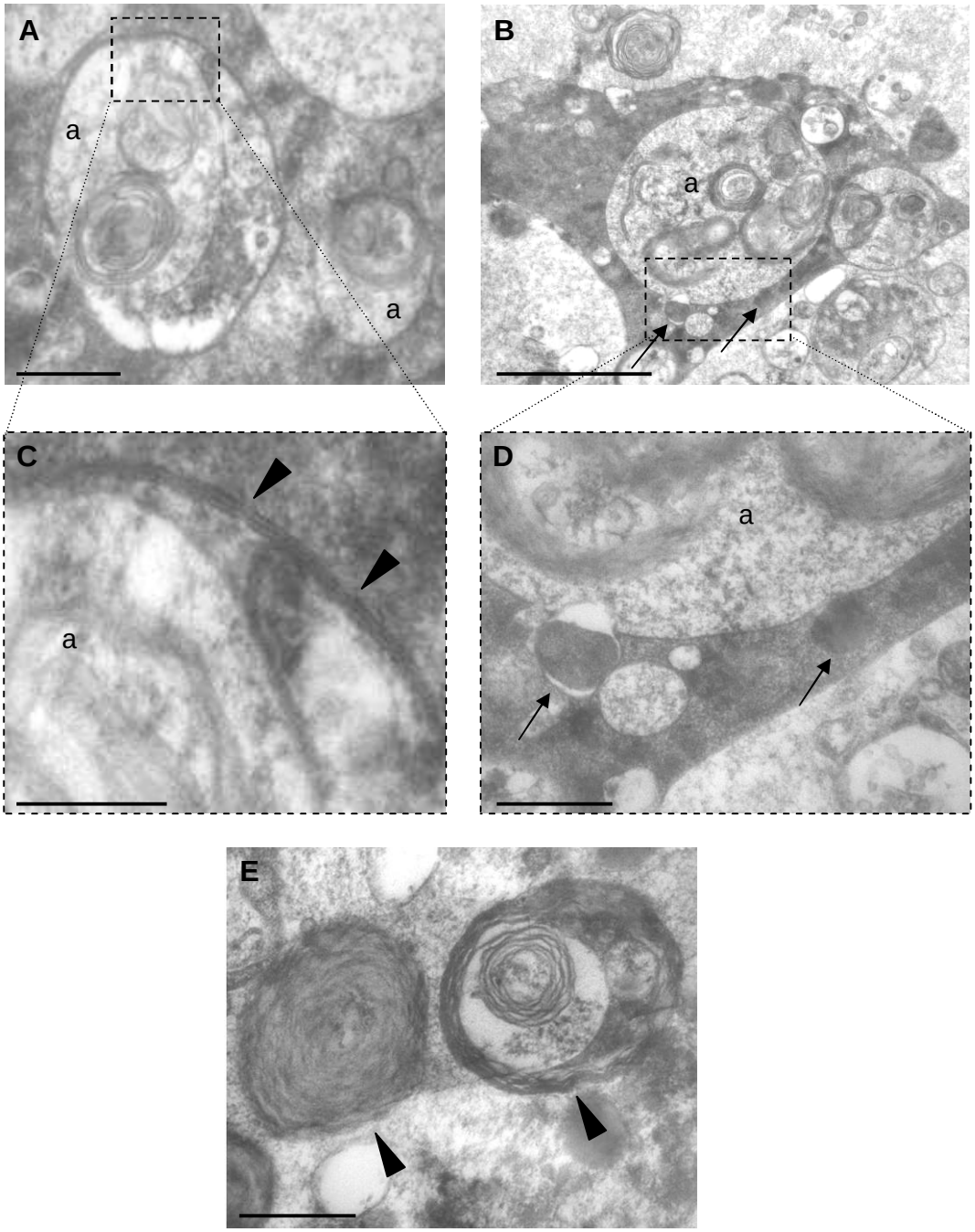
A
a
a
B
a
C
a
D
a
E

Fig. 10 qRT-PCR analysis of autophagy-related genes
High levels of expression for *BmATG5* (**A**), *BmATG6* (**B**) and *BmATG8* (**C**) can be detected at wandering stage. While *BmATG6* and *BmATG8* expression is subjected to a decrease, a second peak of *BmATG5* mRNA can be observed at prepupal stage. Data are represented as Mean ± SE.

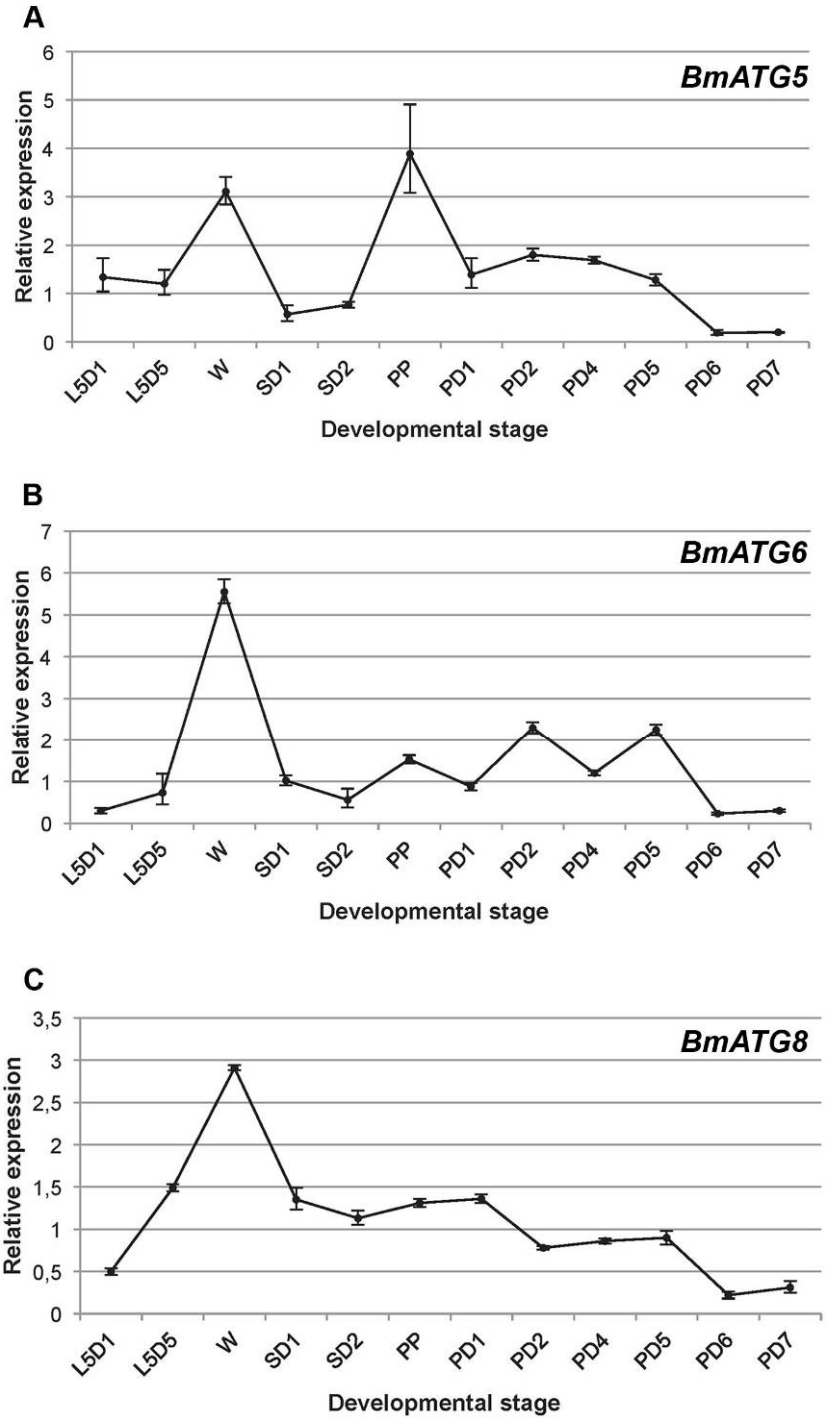
A
BmATG5
Relative expression
0
1
2
3
4
5
6
L5D1
L5D5
W
SD1
SD2
PP
PD1
PD2
PD4
PD5
PD6
PD7
Developmental stage
B
BmATG6
Relative expression
0
1
2
3
4
5
6
7
L5D1
L5D5
W
SD1
SD2
PP
PD1
PD2
PD4
PD5
PD6
PD7
Developmental stage
C
BmATG8
Relative expression
0
0,5
1
1,5
2
2,5
3
3,5
L5D1
L5D5
W
SD1
SD2
PP
PD1
PD2
PD4
PD5
PD6
PD7
Developmental stage

Fig. 11 Expression and localization of BmAtg8 protein
A Western blot analysis of BmAtg8. BmAtg8 antibody recognizes two bands (14 and 12 kDa) from wandering stage onwards. **B-J** Immunolocalization of BmAtg8. The positivity for BmAtg8 is localized in the larval midgut during wandering stage (**B, E, H**). At spinning (**C,F,I**) and pupal stage (**D, G, J**), the signal becomes restricted to the yellowbody. Autophagic compartments are visible as fluorescent dots (**H-J**). **B-D** Reference sections stained with hematoxylin and eosin. **H-J** are details at higher magnification of **E-G**, respectively. *Bracket* indicates the pupal midgut epithelium. *l* lumen, *yb* yellow body. Bars: **B-G** 100 µm; **H-J** 30 µm.

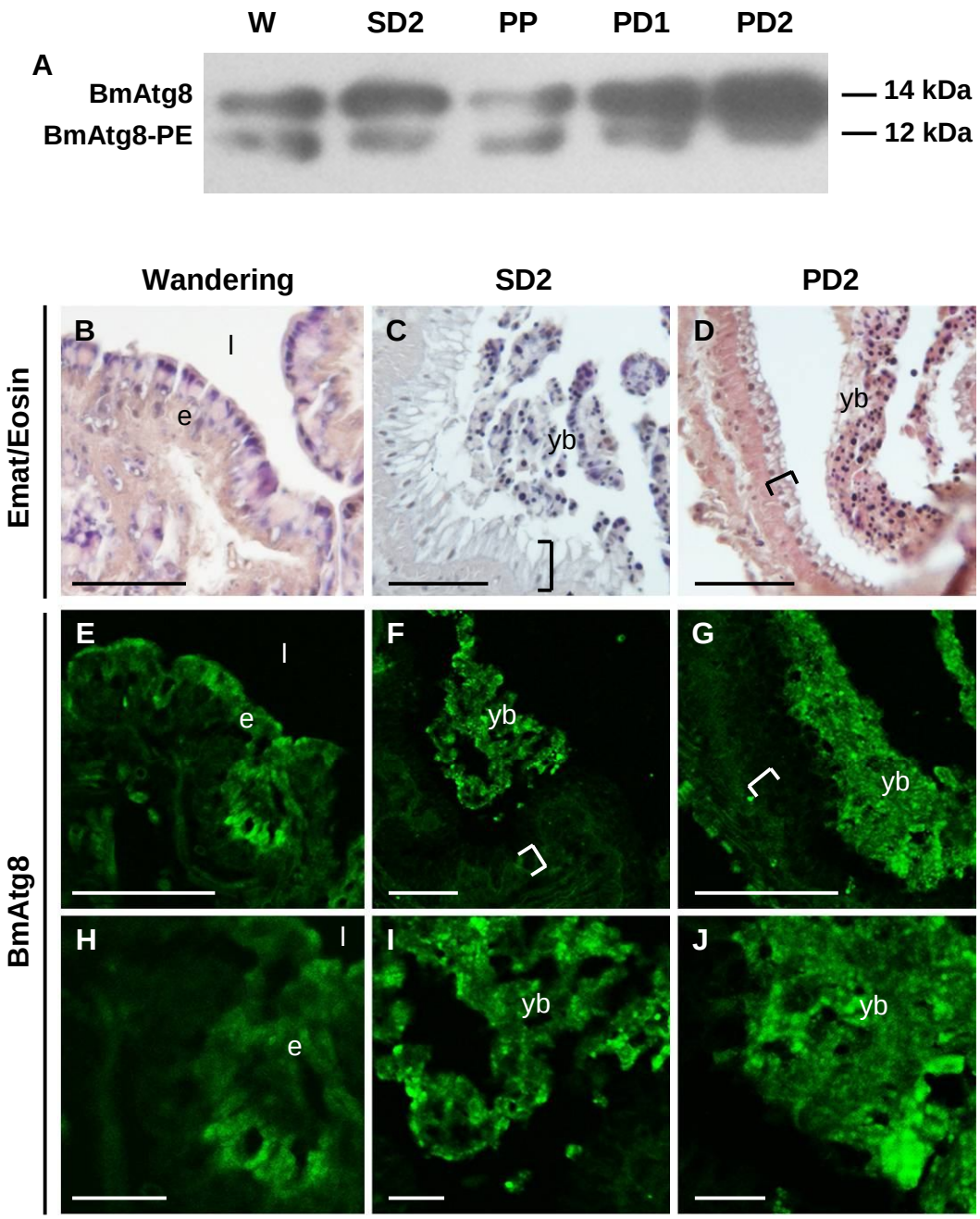
W
SD2
PP
PD1
PD2
A
BmAtg8
BmAtg8-PE
14 kDa
12 kDa
Wandering
SD2
PD2
Emat/Eosin
BmAtg8
B
C
D
E
F
G
H
I
J
l
e
yb

Fig. 12 Analysis of acid phosphatase activity
A The enzymatic assay shows an increase of acid phosphatase activity during the spinning period and a subsequent decrease at prepupal stage. In midgut of pupae the activity is not subjected to high variability. Data are represented as Mean ± SE (n=6) **B-D** The histochemical staining demonstrates that enzyme activity (*red color*) is localized only in the larval midgut epithelium (*e*). Accordingly, from spinning phase onward a strong signal is visible only in yellow body cells (*yb*). *Bracket* indicates the pupal midgut epithelium. **E-G** TEM analysis evidences acid phosphatase activity (*black* reaction product) within cytoplasmic dots (*arrows*) in larval midgut cells. A copresence of acid phosphatase staining and degenerated cell structures can be assessed in some of these corpuscles (*arrowheads*). Bars: **B-D** 100 µm; **E** 2 µm; **F** 500 nm; **G** 200 nm.

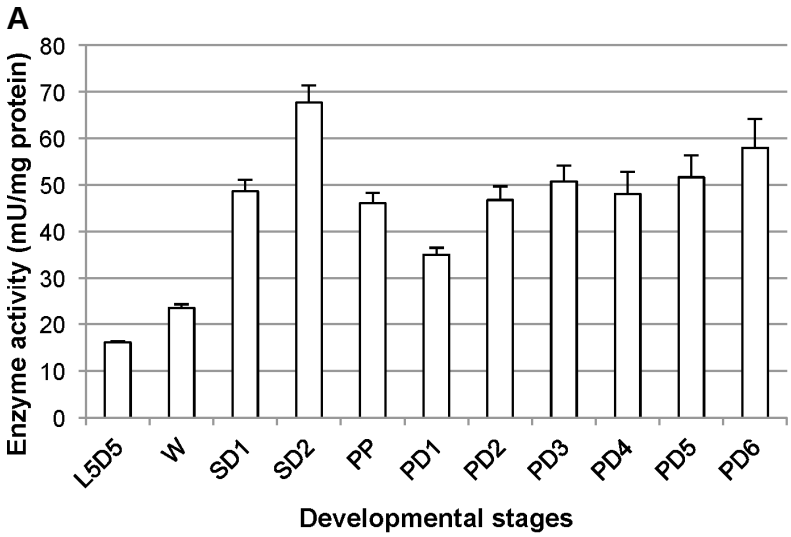
A
Enzyme activity (mU/mg protein)
80
70
60
50
40
30
20
10
0
L5D5
W
SD1
SD2
PP
PD1
PD2
PD3
PD4
PD5
PD6
Developmental stages

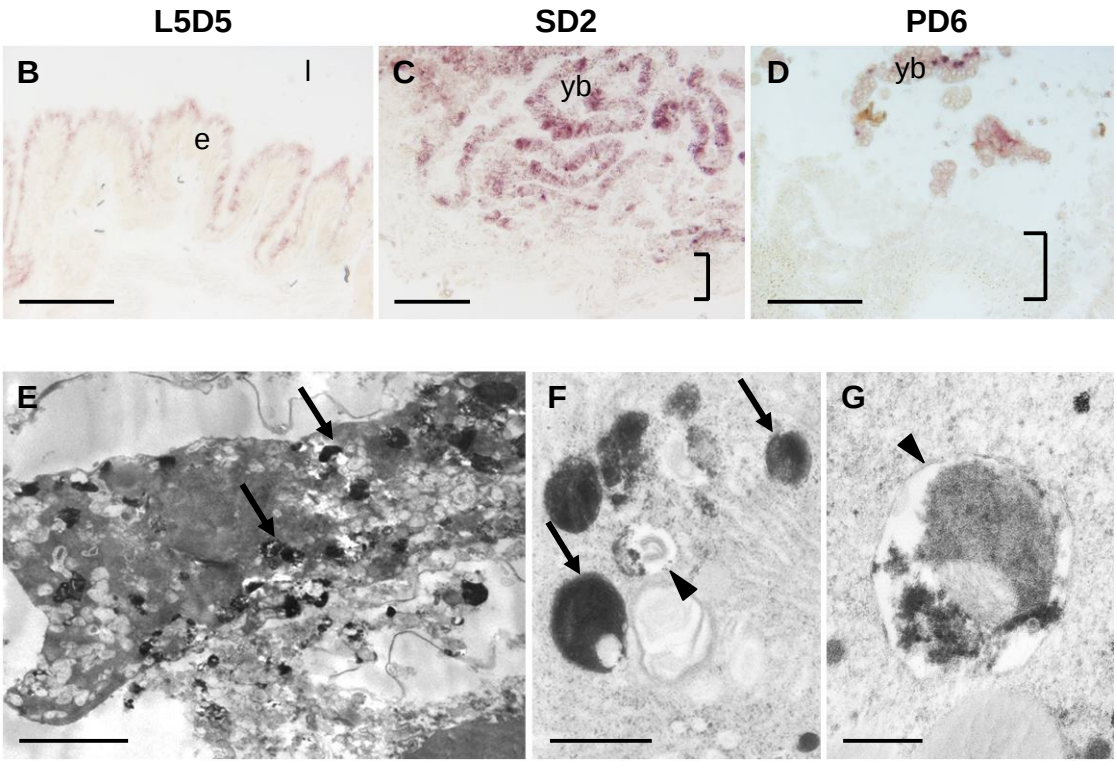
L5D5
SD2
PD6
B
l
e
C
yb
D
yb
E
F
G

Fig. 13 Morphological study of the apoptotic process

Morphological analysis of apoptotic features that can be observed in larval midgut cells from prepupal stage to pupal phase. **A** DAPI staining; **B, C, E,** TEM micrographs; **D** hematoxylin and eosin staining. Nuclear piknosis (*arrowhead*, **A, B**), as well as nuclear fragmentation (*arrows*, **C, D**), are visible in larval midgut cells undergoing degeneration. These apoptotic nuclei are very different from nuclei (*n*) present in midgut cell of fifth instar larvae (**A, D, E**). Bars: **A-D** 10 µm; **B** 5 µm; **C** 1 µm; **E** 2 µm.

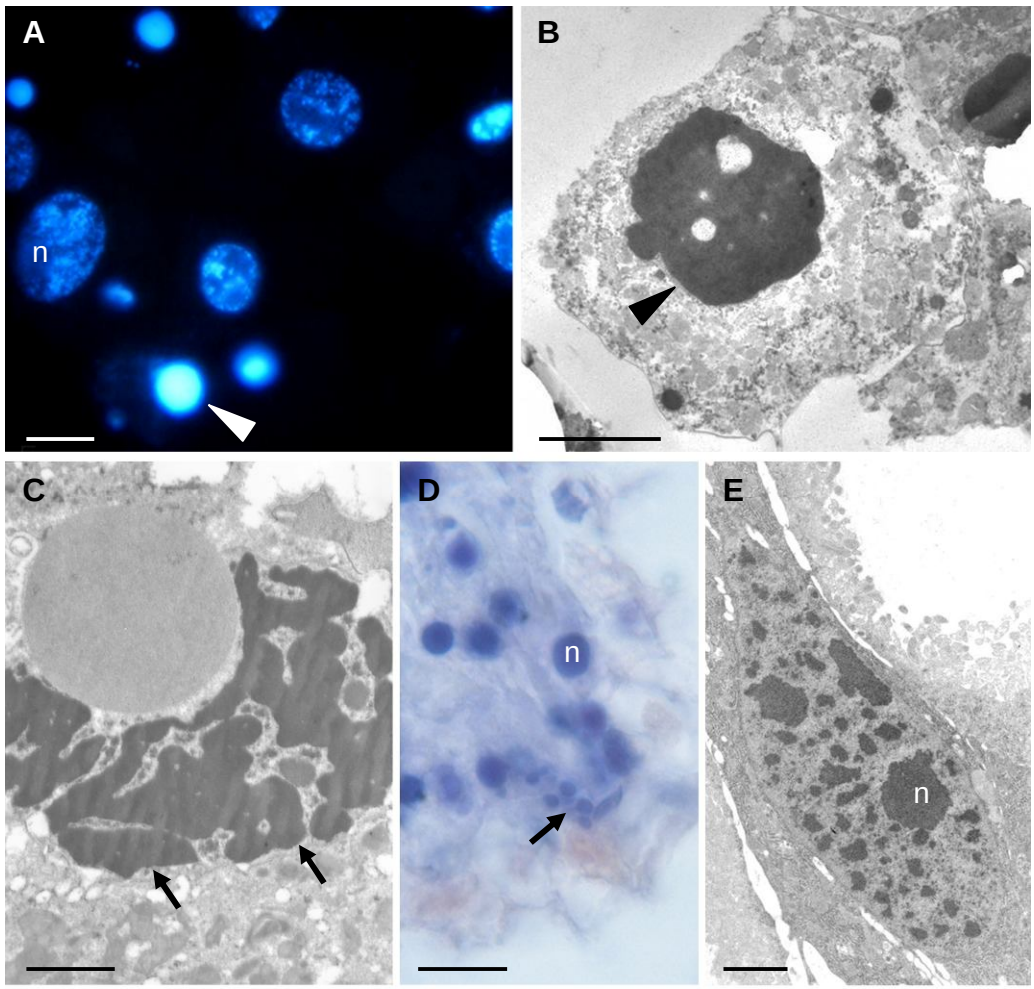
A
n
B
C
D
n
E
n

Fig. 14 qRT-PCR analysis of apoptosis-related genes
High levels of expression for *BmICE-2* (**A**) and *BmCaspase-4* (**B**) are observed during the last day of fifth larval instar (L5D5), followed by a rapid decrease. The expression of the apoptotic inhibitor *BmIAP* (**C**) remains at high levels until wandering stage. Data are represented as Mean ± SE.

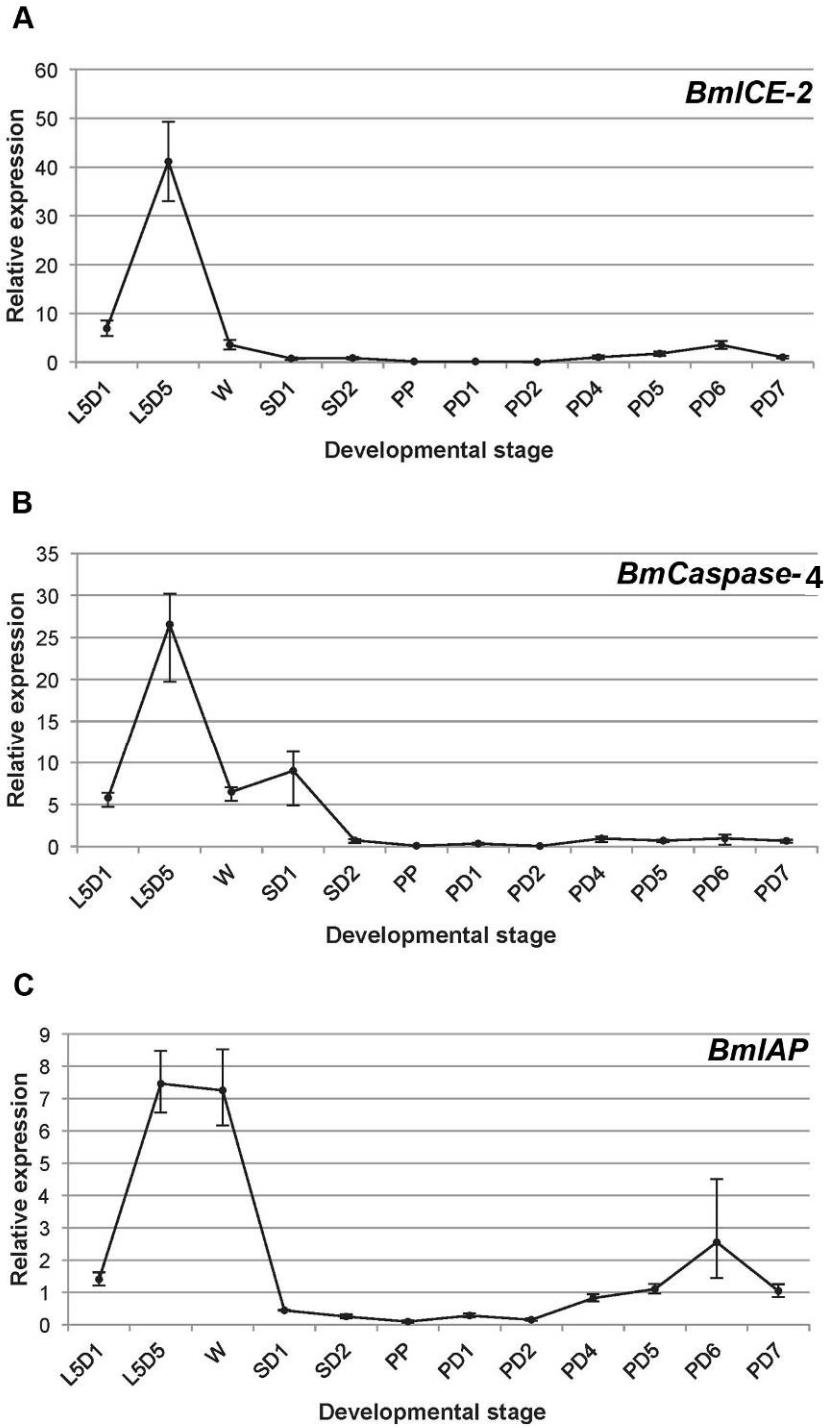
A
BmICE-2
Relative expression
60
50
40
30
20
10
0
L5D1
L5D5
W
SD1
SD2
PP
PD1
PD2
PD4
PD5
PD6
PD7
Developmental stage
B
BmCaspase-4
Relative expression
35
30
25
20
15
10
5
0
L5D1
L5D5
W
SD1
SD2
PP
PD1
PD2
PD4
PD5
PD6
PD7
Developmental stage
C
BmIAP
Relative expression
9
8
7
6
5
4
3
2
1
0
L5D1
L5D5
W
SD1
SD2
PP
PD1
PD2
PD4
PD5
PD6
PD7
Developmental stage

Fig. 15 Analysis of caspase activity

A-H Immunolocalization of activated caspase-3. At larval stage the antibody does not reveal any positivity for caspase-3 (**A, B**), while a signal (*arrowheads*) is visible in cells of the larval midgut epithelium (*e*) at spinning stage (**C, D**). At pupal stage, a strong positivity (*arrowheads*) is found only in cells of the yellow body (**E, F**). No staining can be observed in negative controls (**G, H**). **B, D, F, H** are details at higher magnification of (**A, C, E, G**), respectively. *Bracket* indicates the pupal midgut epithelium. *l* lumen, *yb* yellow body. **I** Western blot analysis of caspase-3. The antibody specific for cleaved caspase-3 recognizes a 15 kDa band, whose intensity is very high at SD2. Positivity for this antibody is also visible in pupal samples. **J** The enzymatic assay shows a massive increase of active effector caspases at SD2. The activity remains high also at pupal stage. Data are represented as Mean ± SE (n=9). Bars: **A, C, E, G** 200 µm; **B, D, F, H** 50 µm.

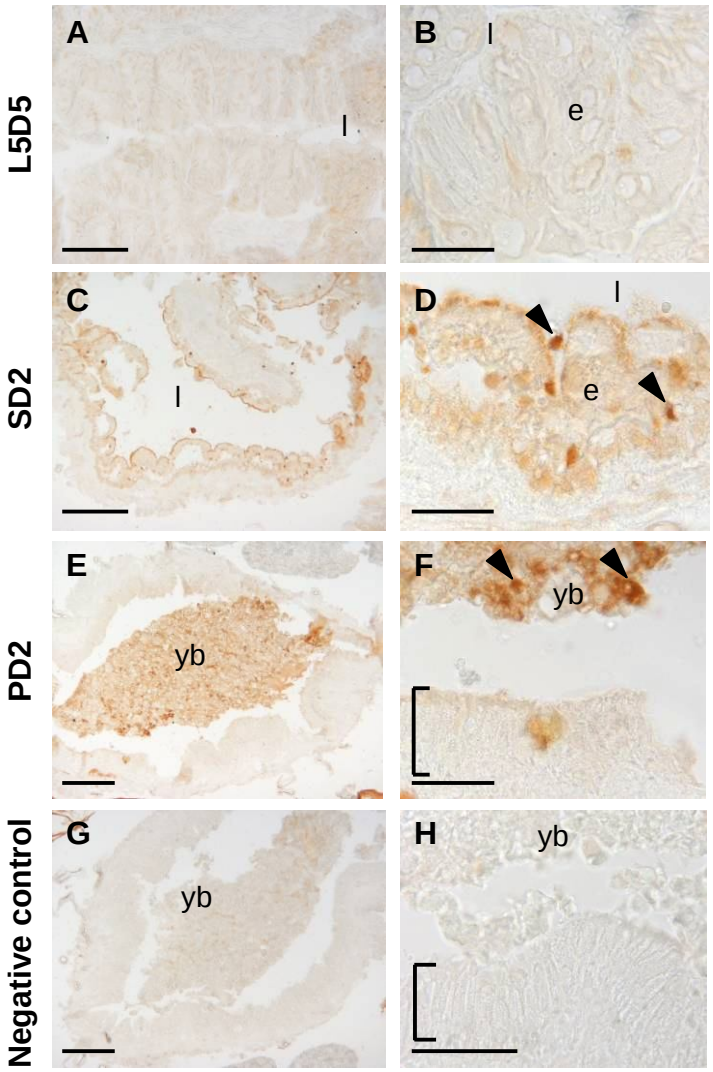
L5D5
SD2
PD2
Negative control
A
B
C
D
E
F
G
H
l
e
yb

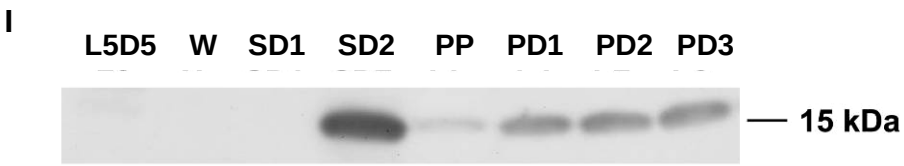
I
L5D5
W
SD1
SD2
PP
PD1
PD2
PD3
15 kDa

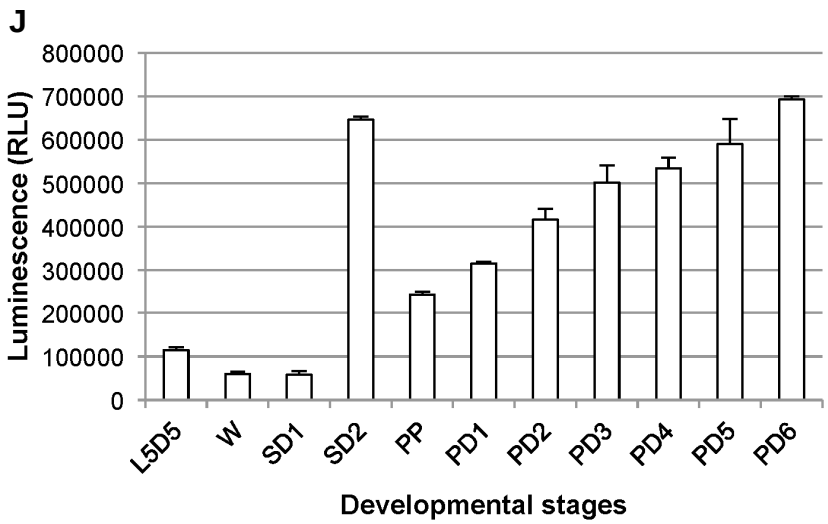
J
Luminescence (RLU)
800000
700000
600000
500000
400000
300000
200000
100000
0
L5D5
W
SD1
SD2
PP
PD1
PD2
PD3
PD4
PD5
PD6
Developmental stages

Fig. 16 Analysis of DNA fragmentation

A-H TUNEL assay. No signal is visible in the midgut epithelium during the fifth larval instar (**A, B**), while a large number of nuclei (*arrowheads*) are stained during spinning (**C, D**) and pupal (**E, F**) stage. No staining can be observed in TUNEL-negative controls (**G, H**). **B, D, F, H** are details at higher magnification of (**A, C, E, G**), respectively. *Bracket* indicates the pupal midgut epithelium. *e* larval epithelium, *l* lumen, *yb* yellow body. Bars: **A, C, E, G** 50 µm; **B, D, F, H** 20 µm

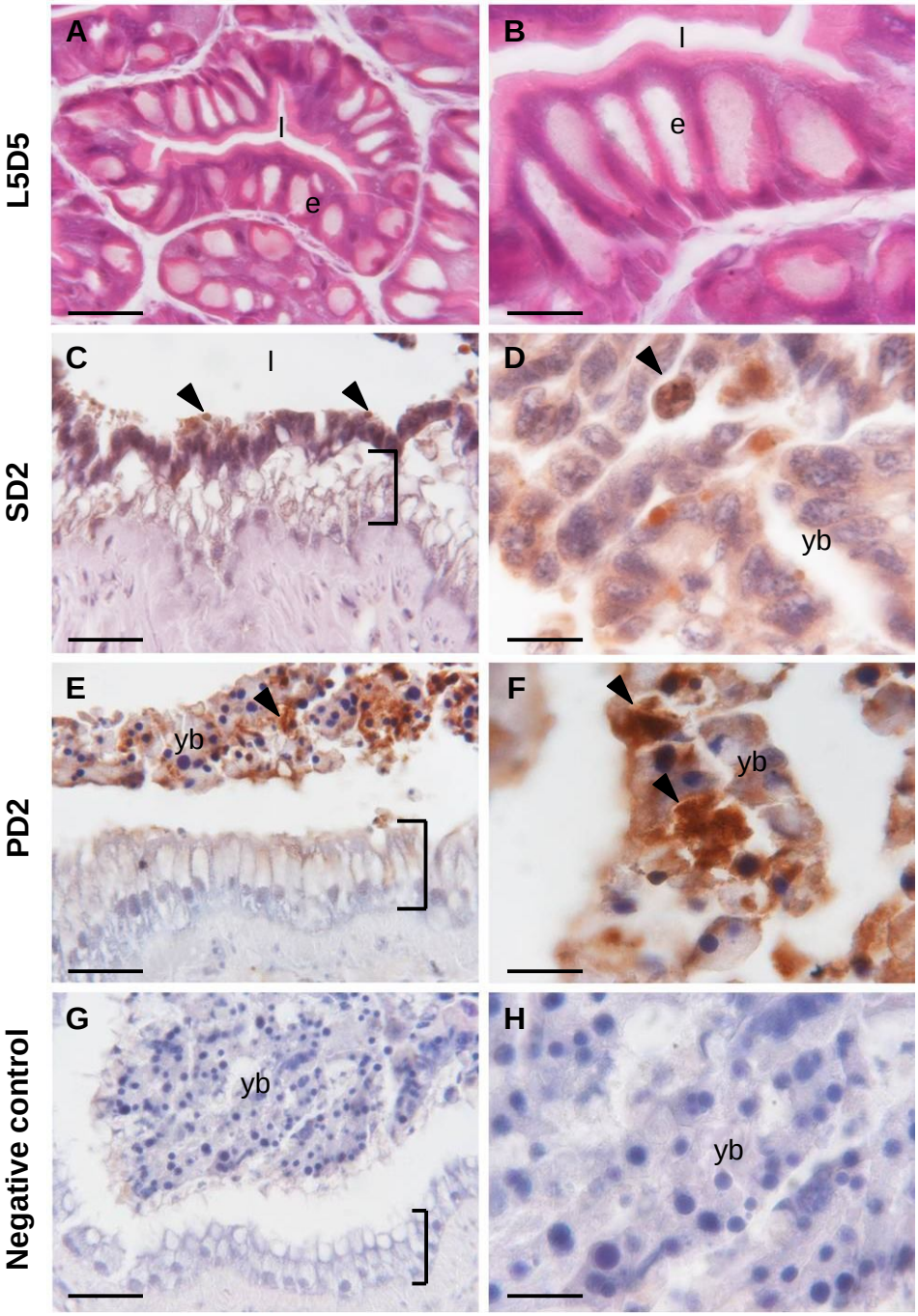
L5D5
SD2
PD2
Negative control
A
B
C
D
E
F
G
H
l
e
yb

Fig. 17 Evaluation of membrane integrity
A-B The treatment of yellow body cells derived from pupal midguts with Ho33258 and PI shows that only some cells are characterized by double staining (*arrow*), a proven indication of membrane damage. Some other cells are characterized only by Ho33258 staining (*arrowhead*). **C** TEM analysis confirms that the membrane of degenerating cells is fragmented (*arrowheads*). *Arrow* indicates plasma membrane. Bars: **A, B** 10 µm; **C** 2 µm.

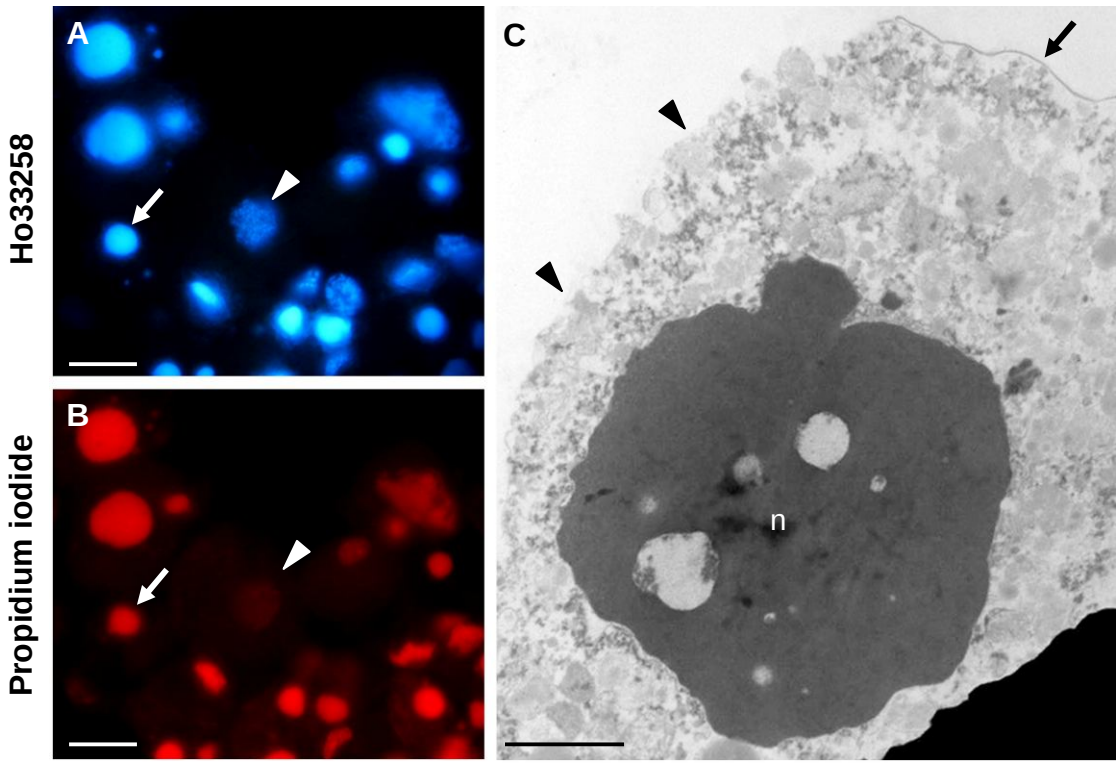
Ho33258
Propidium iodide
A
B
C
n

Fig. 18 Metabolic characterization of midgut epithelium
A Protein content of midgut cells is subjected to a strong decrease starting at wandering stage, when the larva stops feeding. This diminished level of proteins is maintained throughout the whole spinning phase. Data are represented as Mean ± SE (n=9). **B** ATP amount is subjected to a 30-fold increase at SD1 phase, that continues until prepupal phase. Data are represented as Mean ± SE (n=9).

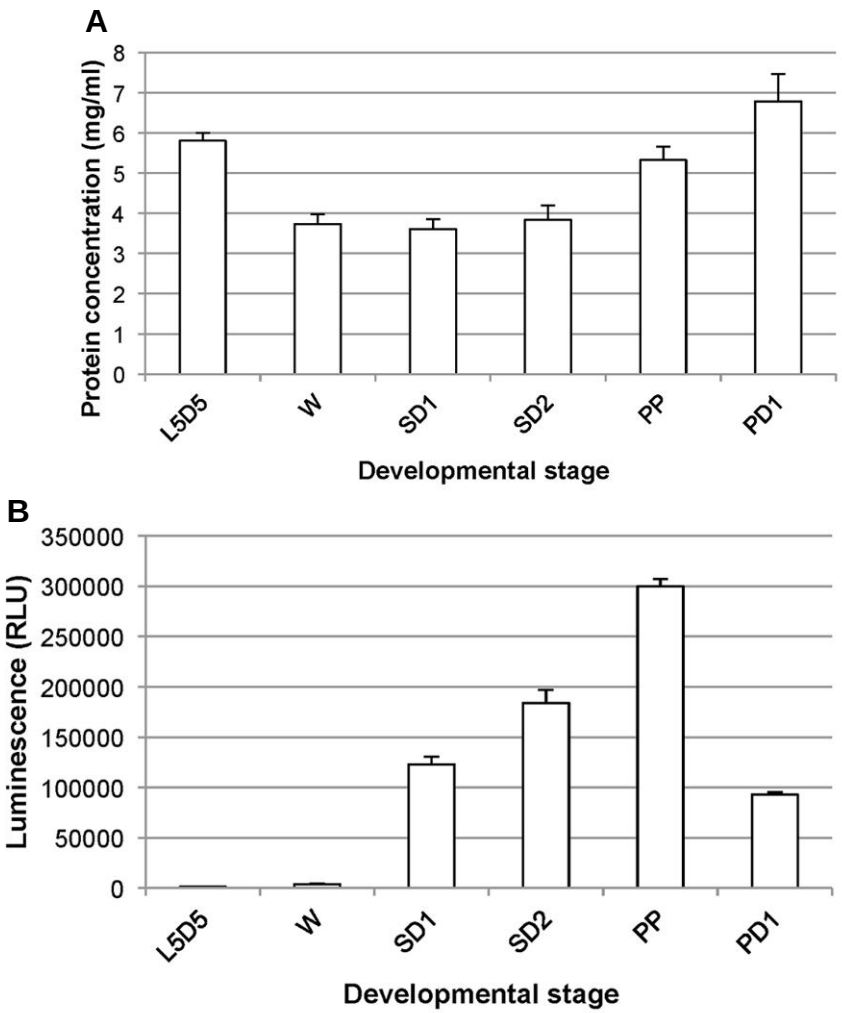
A
Protein concentration (mg/ml)
0
1
2
3
4
5
6
7
8
L5D5
W
SD1
SD2
PP
PD1
Developmental stage
B
Luminescence (RLU)
0
50000
100000
150000
200000
250000
300000
350000
L5D5
W
SD1
SD2
PP
PD1
Developmental stage

Fig. 19 Summary scheme of the most representative cellular, biochemical, and molecular events that occur in silkworm midgut during the period L5D5-PD7

Processes related to autophagy are represented by *blue bars* (*top*), while those referring to apoptosis are represented by *red bars* (*bottom*).

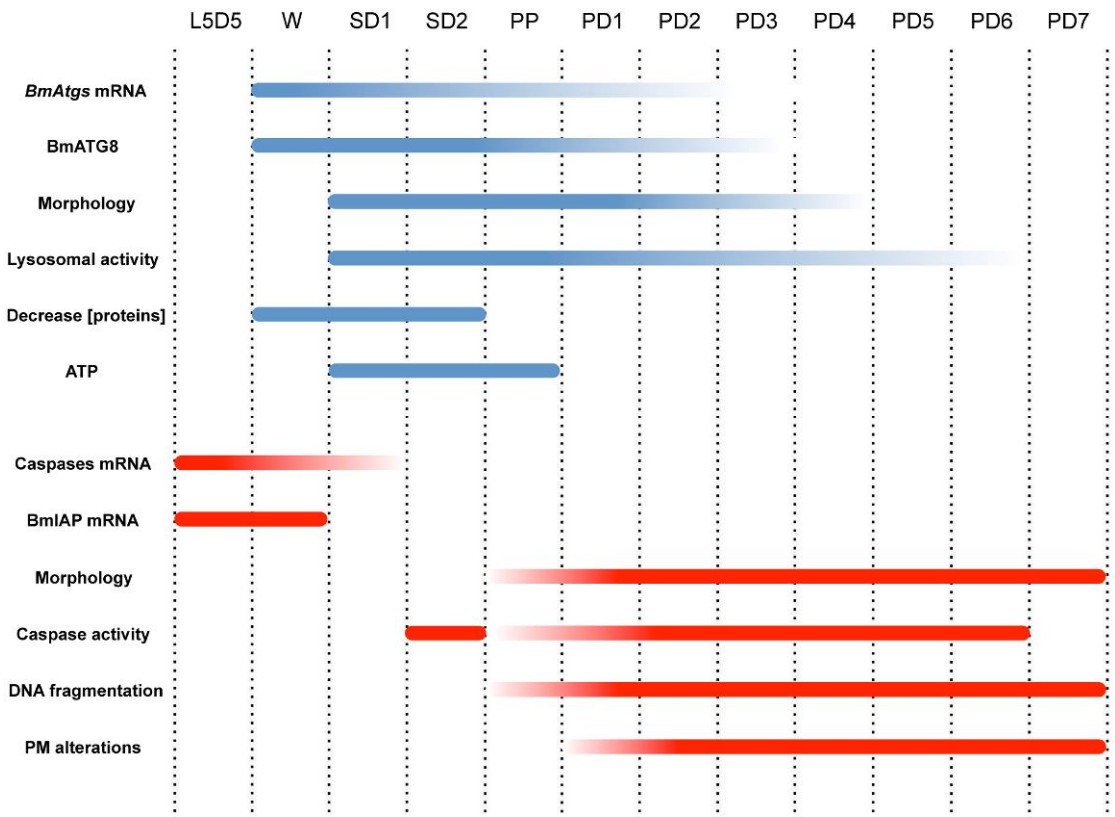
L5D5
W
SD1
SD2
PP
PD1
PD2
PD3
PD4
PD5
PD6
PD7
BmAtgs mRNA
BmATG8
Morphology
Lysosomal activity
Decrease [proteins]
ATP
Caspases mRNA
BmIAP mRNA
Morphology
Caspase activity
DNA fragmentation
PM alterations